museum

INSTITUT ROYAL DES SCIENCES NATURELLES DE BELGIQUE
KONINKLIJK BELGISCH INSTITUUT VOOR NATUURWETENSCHAPPEN

ROYAL BELGIAN INSTITUTE OF NATURAL SCIENCES

MEMOIRS OF THE GEOLOGICAL SURVEY OF BELGIUM
N. 58 - 2012

GRAVITY ACQUISITION IN BELGIUM AND THE RESULTING BOUGUER ANOMALY MAP

MICHEL EVERAERTS & WALTER DE VOS

SERVICE GEOLOGIQUE DE BELGIQUE
BELGISCHE GEOLOGISCHE DIENST

Geological Survey of Belgium

Rue Jenner 13 - 1000 Bruxelles
Jennerstraat 13 - 1000 Brussel

ISSN 0408-9510

KONINKLIJK BELGISCH INSTITUUT
VOOR NATUURWETENSCHAPPEN

INSTITUT ROYAL DES SCIENCES
NATURELLES DE BELGIQUE

ROYAL BELGIAN INSTITUTE OF NATURAL SCIENCES

GEOLOGICAL SURVEY OF BELGIUM
MEMOIRS of the GEOLOGICAL SURVEY OF BELGIUM N° 58 - 2012

GRAVITY ACQUISITION IN BELGIUM AND THE RESULTING BOUGUER ANOMALY MAP

Michel EVERAERTS & Walter DE VOS

Cover illustration: the practice of gravity measurements in Belgium

Table of contents **Error! Bookmark not defined.**

[m1]

GRAVITY ACQUISITION IN BELGIUM AND THE RESULTING BOUGUER ANOMALY MAP

Michel EVERAERTS & Walter DE VOS

Royal Belgian Institute of Natural Sciences - Geological Survey of Belgium
Jenner str. 13, B-1000 Brussels
michel.everaerts@naturalsciences.be walter.devos@naturalsciences.be

Manuscript received 24.6.2011; accepted for publication 18.11.2011.

Abstract. The present memoir has two main aims: to document the work done in gravimetric data acquisition in Belgium, going back to the nineteenth century, and to calculate and discuss a new Bouguer anomaly map based on a novel approach with a varying reduction density. Gravity measurements have three main applications: metrology (to locally calibrate instruments such as balances), geology (to understand the local subsoil at varying depths), and geodesy. The first chapter of the memoir places the Belgian part of the geoid in the framework of a general presentation of the world geoid. It is used to locate oneself with GPS in altitude with a precision of 2 cm, the Belgian geoid being one of the most detailed in the world because of the very high gravity coverage. Some theoretical considerations concerning gravity measurement, and the realisation of modern networks, are presented in the second and third chapters respectively. Since geological interpretation of the Bouguer anomaly map is the main concern of the geological community, the fourth chapter gives an overview of the history of gravity acquisition in Belgium and the related evolution of the Bouguer map, giving some short biographical notes about scientists who intensively participated in the gravity acquisition. The fifth chapter discusses the development of a new Bouguer map calculated with varying reduction density, adapted to the Belgian subsoil. To reach this goal it was necessary to make use of the bathymetric map of the Palaeozoic and the topographic map of the younger unconsolidated cover rocks. The last chapter is concerned with the geological interpretation of the spatial variation of gravity in Belgium, and discusses both the existing scientific literature and the peculiarities of the new Bouguer anomaly map produced in 2011 (this work).

Samenvatting. **Gravimetrische opname van België en de Bouguer-kaart**. In deze verhandeling worden twee hoofddoelstellingen gesteld: enerzijds het documenteren van het geleverde werk op het gebied van gravimetrische data-acquisitie in België sinds de 19e eeuw, en anderzijds het maken van een nieuwe Bouguer-kaart met een variabele reductiedichtheid. Metingen van de zwaartekracht hebben drie toepassingsdomeinen: de metrologie (voor het lokaal ijken van toestellen zoals weegschalen), de geologie (voor het begrijpen van de lokale ondergrond op verschillende diepte) en de geodesie. In het eerste hoofdstuk van deze verhandeling wordt het Belgische deel van de geoïde geplaatst binnen een algemene voorstelling van de globale geoïde. Deze wordt gebruikt om zich met GPS met een precisie van 2 cm te positioneren in de hoogte. Dit is één van de meest gedetailleerde modellen ter wereld gezien de zeer hoge densiteit van de gravimetrische bedekking van België. De tweede en derde hoofdstukken handelen over theoretische overwegingen betreffende zwaartekrachtmetingen, en over de wijze waarop moderne netwerken gerealiseerd worden. Aangezien de geologische interpretatie van de Bouguer-kaart steeds de belangrijkste bekommernis is van de geologische gemeenschap, wordt in het vierde hoofdstuk een overzicht gegeven van de geschiedenis van de gravimetrische metingen in België, en de daaraan gekoppelde evolutie van de Bouguer-kaart, met enkele korte biografische nota's over personen die intensief deelgenomen hebben aan acquisitie van terreingegevens. Het vijfde hoofdstuk behandelt het opstellen van een nieuwe Bouguer-kaart met variabele reductiedichtheid, aangepast aan de specifieke Belgische ondergrond. Hiervoor was het noodzakelijk om een bathymetrische kaart van het Paleozoïcum en een topografische kaart van de jongere afdekkende lagen te betrekken bij de berekeningen. Het laatste hoofdstuk is gewijd aan de geologische interpretatie van de ruimtelijke variatie van de zwaartekracht in België, en behandelt zowel de bestaande wetenschappelijke literatuur als de kenmerken zichtbaar op de nieuwe kaart van de

Bouguer-anomalie anno 2011 (dit werk).

Résumé. Levé gravimétrique de la Belgique et la nouvelle carte de Bouguer. Ce mémoire a deux objectifs principaux: d'une part documenter le travail réalisé pour l'acquisition des données gravimétriques belges de terrain depuis le XIXe siècle, et d'autre part la réalisation d'une nouvelle carte de Bouguer calculée avec une densité de réduction variable. La gravimétrie a trois principaux domaines d'application : la métrologie (pour la calibration locale d'appareils tels que des balances), la géologie (pour comprendre le sous-sol local à différentes profondeurs) et la géodésie. Dans le premier chapitre de ce mémoire, nous présentons le géoïde de Belgique dans le cadre du géoïde mondial. Celui-ci est utilisé pour se positionner en altitude avec les GPS avec une précision de 2 cm ; en Belgique, il est un des meilleurs du monde grâce à la grande densité de la couverture gravimétrique belge. Les deuxième et troisième chapitres présentent des considérations théoriques sur la gravimétrie et la manière de réaliser des réseaux modernes. Comme l'interprétation géologique de la carte de Bouguer est une préoccupation majeure de la communauté géologique, nous présentons dans le quatrième chapitre un historique des mesures gravimétriques en Belgique, l'évolution de la carte de Bouguer dans le temps, ainsi que des courtes notes biographiques sur les personnes intensivement impliquées dans l'acquisition des données de terrain.
Le cinquième chapitre expose ce qui a été mis en œuvre pour réaliser une carte de Bouguer avec une densité de réduction variable. Pour atteindre ce but, il a été nécessaire d'impliquer dans les calculs la carte bathymétrique du Paléozoïque et la carte topographique de la couverture plus jeune. Le dernier chapitre est consacré à l'interprétation géologique de la carte de Bouguer belge, et inclut une revue de la littérature scientifique ainsi que l'interprétation des caractéristiques de la nouvelle carte de 2011 (ce travail).

Acknowledgements
The Geological Survey of Belgium and the Royal Observatory of Belgium have allowed the present gravimetric work to proceed over the last few decades in a spirit of scientific collaboration. The National Geographical Institute, in particular the geodesy department, carried out a large part of the field work over many years. The regions: Flanders, Wallonia and Brussels, participated in the financing of this ambitious project. The authors wish to thank Paul Pâquet and Pierre Keating for reviewing and improving the manuscript.

1. Introduction: gravity and the geoid

The value of gravity at the surface of the earth is slightly different according to the particular location where it is measured. Belgium has a tradition of gravity measurements going back to the end of the nineteenth century, as will be explained in chapter4. Why are we interested in the precise value of gravity, "small g", in a particular place? There are three main applications. First, the value of g is used in metrology to allow the calibration of pressure instruments and balances. Second, it is used in geodesy to calculate the geoid, and in altimetry reference systems relying on Global Positioning System satellites. Finally it is used in geology as an indirect way to access the composition of crustal rocks, in areas with poor outcrops or as a continuation at depth of shallow structures. The variation of gravity at the surface of the earth is closely related to the density of the rocks. The present publication will investigate the geological causes of the gravity variation in Belgium, in chapter 6. But in order to define a broad framework for gravity measurements, we will start by describing the geoid.

1.1. The Geoid

The **geoid** is an equipotential surface corresponding to the mean ocean surface of the earth. It comes closer to describing the real shape of the earth than the spherical or ellipsoidal approximation. The geoid, also called "gravity geoid", represents sea level, i.e. the surface of the earth in gravimetrical equilibrium; under land areas this is where the water surface would be if extended from sea areas. We can determine the local shape of the geoid with less or more accuracy, so there is more than one version of the geoid.

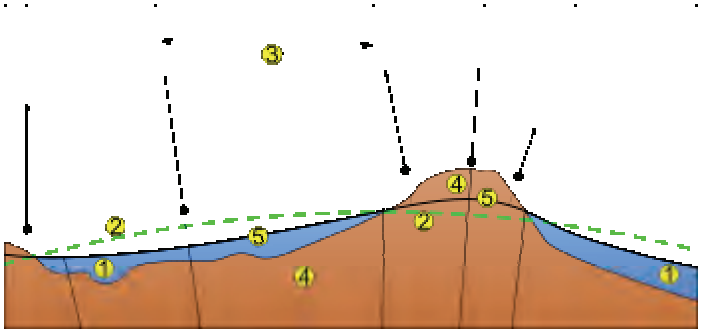

Figure 1. Construction of the geoid. 1. Sea level. 2. Ellipsoid. 3. Plumb lines. 4. Topography/bathymetry. 5. Geoid.

On earth, each point feels a gravity acceleration g. This acceleration derives from the gravitational potential W such thatg=grad(W). A surface where the gravity potential W is constant is a gravity equipotential surface. And the geoid is the equipotential surface nearest to the mean sea level.

In figure 1, the reference ellipsoid (2) is a regular geometric body with the shape of a flattened sphere. Actual sea level (1) deviates from this ellipsoid; it corresponds to the geoid (5) and can be extended under continental areas. The gravity acceleration is a vector perpendicular to the geoid, represented by the plumb lines (3), which define the local vertical. The land surface (4) defines topography above sea level and bathymetry below sea level. The geoid looks like a distorted ellipsoid. It does not coincide with the ellipsoid because of the unequal repartition of mass inside the earth. The occurrence of a mountain belt, for instance, will create a visible distortion on the geoid surface. Dense basaltic rocks surrounded by lighter sedimentary rocks will also create a visible distortion.

1.2. The height or altitude

A height expresses the vertical distance between a point and the geoid, also called MSL, or *Mean Sea Level* . As the ellipsoid and the geoid do not coincide, the difference between the two is called the geoidal height, and it can reach a value of 100 m.

The topographic height H, above sea level, is the same as the orthometric height, and in Belgium in some points it has been measured twice at the location of the benchmarks. The first measurement was made with a classical levelling using theodolites on the ground, which established first a topographic height. Later, a GPS (Global Positioning Satellites) measurement was made in these same points, an operation which determines the ellipsoidal height (h) with respect to an ellipsoid model presently known as WGS84, because the ellipsoid is the reference system of the GPS satellites. The difference between topographic height and ellipsoidal height is the geoidal height. The benchmarks where both measurements were carried out will be called the "levelled GPS points" further on.

In an unknown point (for instance a new gravity acquisition point), to convert ellipsoidal height (h) (obtained from a GPS measurement) to orthometric height(H), two methods can be used:

- We can establish a local geoid by determining the ellipsoidal height of a few levelling benchmarks or geodesy points, determine the corresponding geoidal heights, and interpolate the geoid to the unknown point.
- Or we can use the national geoid model, which was adapted to the levelled GPS points (as explained above).

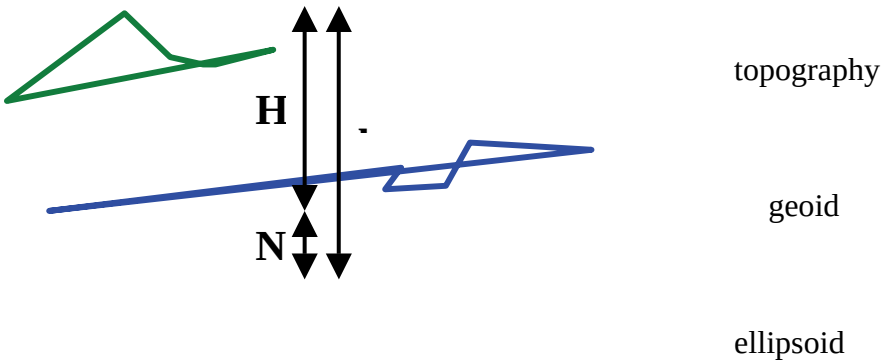

H= orthometric height, relative to sea level

h = ellipsoidal height, as measured with GPS

N = geoidal height

Figure 2. Scheme defining ellipsoidal, geoidal and orthometric height of an observation point.

Only the first method was used until the middle of the nineties (1990), because at that time precise geoid models were missing. But there is a certain error. If we compute a local geoid on the basis of levelled GPS points, small ripples or errors of one to two centimeters will be noticed. This method produces altimetric points with different levels of accuracy, with the disadvantage that it is impossible to compare them.

The other method consists in first producing a geoid model covering the whole country accurately enough to meet the need for levelling by GPS in terms of accuracy, resolution and reliability. The recent progress in the field of geoid modelling, data collection, and computer power, enables this approach in countries with a solid geodesic base. In 1996 two solutions were calculated for Belgium and Luxembourg, one by the Formula of Stokes and the other one by collocation (Pâquet et al., 1997). The accuracy was estimated with the help of 36 levelled GPS points. The error was around 3-4 cm in most of the country, but 14 cm in Arlon (the Ardennes were poorly covered). In 2003 with the help of the new data (New Global field model, new digital terrain model, new gravity data, GPS levelled points), a new computation was realised (Barzaghi et al., 2003).

1.3. The gravimetric geoid or gravity geoid

Nowadays the GPS is widely used to obtain a position in φ, λ and H, but a problem is that the H from the GPS is referenced to the ellipsoid WGS84 and not to any national altitude system. As we have seen before, altimetry and geoid are linked. To transform ellipsoidal height to orthometric height, we have to know the local variation of the geoid (see fig. 2). Figure 3 shows the geoidal height over the territory of Belgium, as the deviation with respect to the ellipsoid, which is the regular geometric figure.

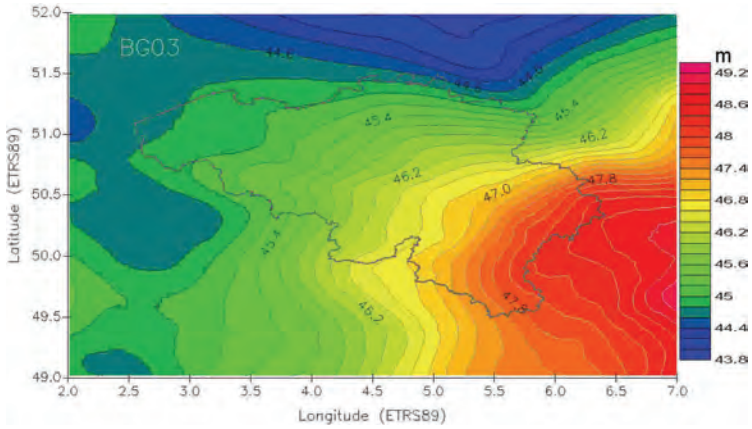

Figure 3. Map of the Belgian Geoid BG03 (2003), in meters above the reference ellipsoid WGS84.

1.4. Altitudinal Reference

When a user realises a levelling with the GPS, he hopes to achieve the same result as with classical levelling, reachingan accuracy of a few centimeters. However, t**he gravity geoid cannot be used directly** to convert the ellipsoidal height to orthometric height. There are numerous reasons for this:

- The geodesy references (benchmarks and ellipsoids used) of the GPS network and the geoid may be different, and the differences are not well known.
- The coefficients of the global field model used can have errors, and if the gravity coverage is not dense enough it will not be correct.
- There are systematic errors in the gravity measurements (wrong calibration of the gravimeter, errors in the processing of the data) or accidental errors.
- The method used to calculate the geoid is not rigorous enough.
- GPS can have a local error (due to tropospheric and ionospheric effects for example).
- Non-measurement of the antenna height of the GPS device can cause errors.
- The altitude of the fundamental benchmark of the classical levelling network may be different from the reference of the geoid.
- The classical ground-based levelling network may have a systematic error.

One can say that the global field model, the gravity measurements and the DTM (digital terrain model) on the one hand, and the geodesy and levelling networks on the other hand, lead to two different geoids. The user has to connect his local network to the legal references, but the points measured inside a local network mostly are not dense enough and can have errors. The gravity geoid acts as an interpolator but it has to be put into a reference, validated and corrected. A reference usable for the levelling by GPS can be obtained by fitting (adapting) the gravimetric geoid to the total number of levelled GPS points representative of the geodesy and altimetry references which should remain unchanged. Figure 4 is a map of all levelled GPS points in Belgium. This set of geodesy points is defined in ellipsoidal coordinates (with respect to WGS84), in orthometric height referring to DNG-TAW (Deuxième Nivellement Général - Tweede Algemene Waterpassing) and also in horizontal reference. These points have been used to calculate the correction map HBG03 shown in figure 5.

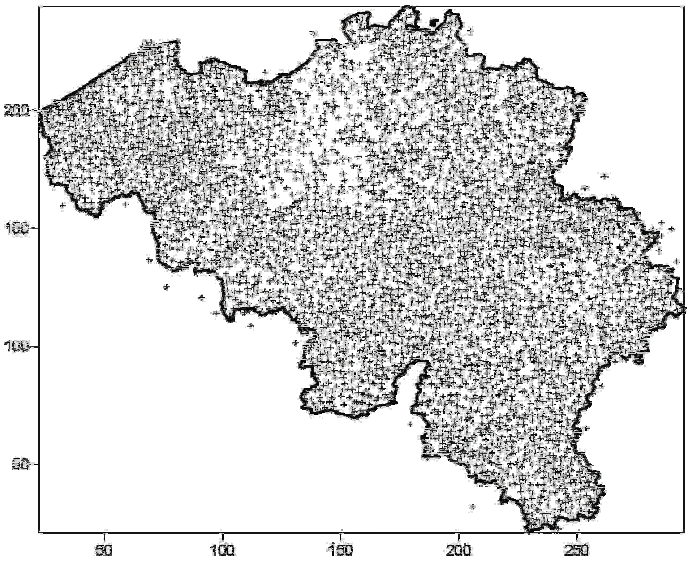

Figure 4. The 4000 levelled GPS points measured by the NGI (National Geographic Institute).

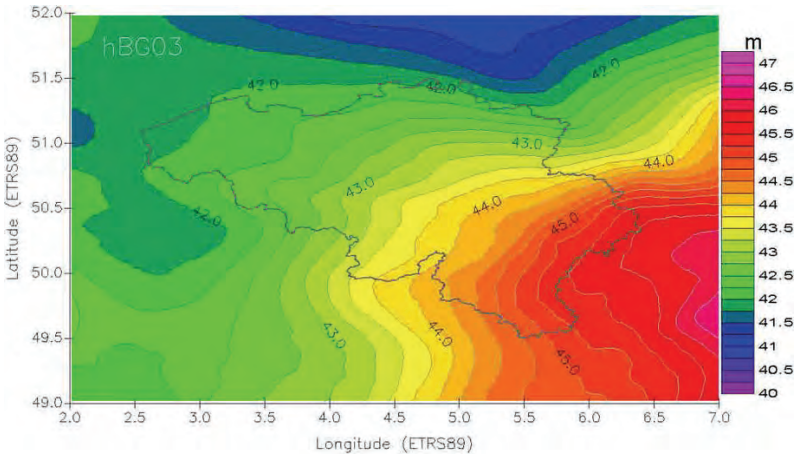

Figure 5. Final correction map HBG03 used to correct the altitude of a GPS point.

1.5. Conclusion for the Belgian geoid

The comparison of the model obtained with levelled GPS points allows us to estimate the accuracy of the computing methods and a cross-validation of the data (gravity, altimetry, and height of the GPS points). Since we have a huge number of levelled GPS points it was possible to transform the geoid into an operational and reliable altidudinal reference, HBG03 (Duquenne et al 2005). The levelling with GPS alone is now possible in Belgium with an accuracy of 2 cm. This covers most of the needs.

1.6. The geoid of the world

Figures 6 and 7 show geoid images collected by the European GOCE satellite. This satellite was launched in March 2009 and has now collected more than 12 months of gravity data. ESA's GOCE mission has delivered the most accurate model of the geoid ever produced, which will be used to further our understanding of the inner workings and structure of the earth. The colours in the image represent deviations in height (–100 m to +100 m) from an ideal geoid. The blue colours represent low values and the reds/yellows represent high values. In figure 6, the deviation of the shape of the earth from a perfect sphere has been strongly exaggerated to enhance the effect.
A precise model of the Earth's geoid is crucial for deriving accurate measurements of ocean circulation, sea-level change and terrestrial ice dynamics. The geoid is also used as a reference surface

from which to map the topographical features on the planet. In addition, a better understanding of variations in the gravity field will lead to a deeper understanding of Earth's interior, such as the physics and dynamics associated with volcanic activity and earthquakes.
Credits: ESA (European Space Agency)/HPF/DLR

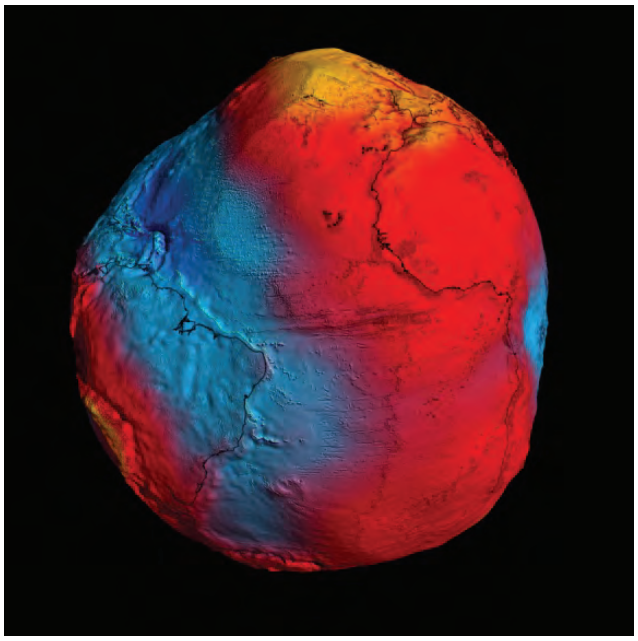

Figure 6. The World gravity geoid (after 2 years' observations by the GOCE satellite). Deviation from sphere is strongly exaggerated.

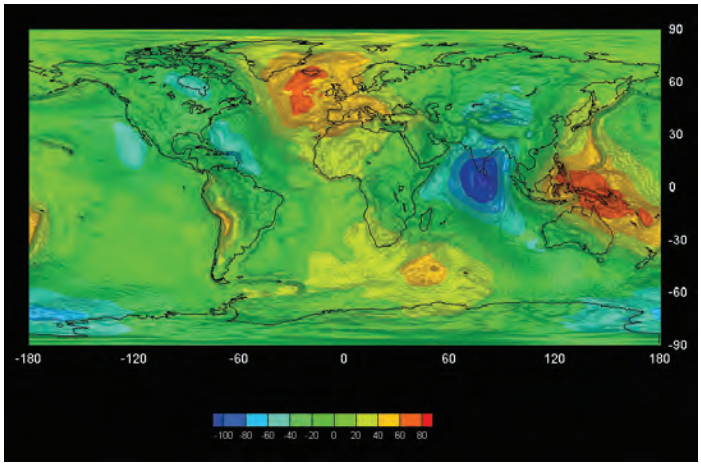

Fig. 7. Map of the geoid after 2 months' measurements by the GOCE satellite. Height in meters.

2. Theoretical considerations

1.7. Gravity[m2] acceleration

The earth's gravity acceleration g is the result of the Newton attraction force Fa on a body and the centrifugal force Fc due to the earth's rotation. The resultant force is Fr=Fa+Fc=M*g where M is the body mass. The average value at the latitude of Belgium is 981 gals(1 gal equals 1 cm/s² in cgs units, and this unit is called gal in honour of Galileo; the symbol is Gal with a capital letter). It varies from 978 gals at the equator to 983 gals at the poles. The geologist is mostly interested in density variations in the crust and in the mantle, which translate to regional gravity variations in the order of 100 mGal or 1/10 000th of the observed value of 981 gals (also expressed as 981 cm/s² or 9.81 m/s²). The accuracy needed to solve geological problems or model structures is in the order of 0.1 to 1 mGal.

1.8. The Instruments: gravimeters

There are two kinds of gravimeter :

- Relative gravimeters are instruments that allow networks to be built (LaCoste-Romberg G and D, or Scintrex gravimeters). Each measurement is a Δg i.e. a difference between two consecutive measurements, generally expressed in m/s².Every measurement is tied to its neighbours.
- The absolute meters give reference points or standards. This measurement is expressed in g and is a value between 9.78 and 9.82.

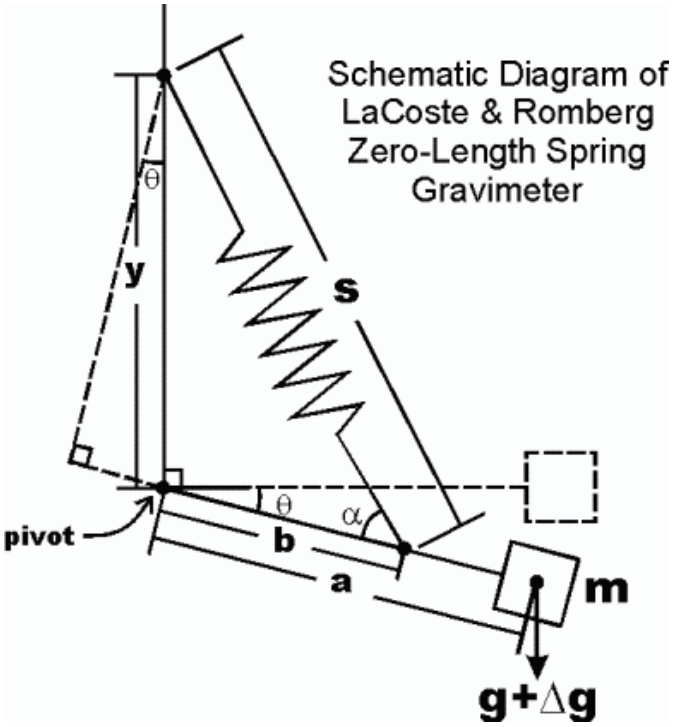

Figure 8. Scheme of the LaCoste- Romberg gravimeter in the vertical plane.

The LaCoste-Romberg gravimeter (figure 8) is astatised[1] to give more sensitivity to the measurement. A horizontal beam carries a mass on one side, while at the other side it is attached in such a way that it can rotate in the vertical plane around a horizontal axis. The beam is linked with a spring to a vertical beam above the rotation point. It rotates (the mass goes down) with an increase in gravity; the length of the spring increases and the angle α between the spring and the beam decreases. A reading is performed by setting the beam back to the horizontal position with a null dialling screw.

[1] Astatised : the centre of gravity is eccentric to the rotation axis. This increases the sensitivity of the instrument.

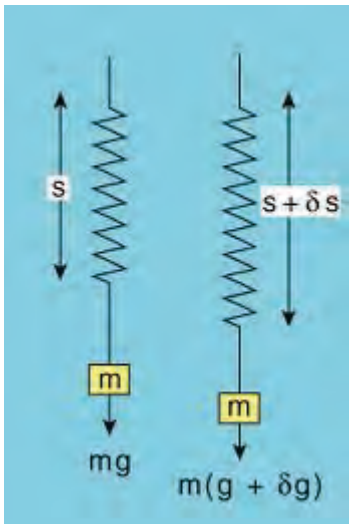

Figure 9. Vertical scheme of a Scintrex gravimeter.

In a Scintrex gravimeter (figure 9) a metal mass hangs freely from a spring. This spring is elongated when gravity is stronger. The position of the spring is converted into an electrical signal (*voltage difference ΔV)* proportional to the gravity intensity.

In an absolute gravimeter (figure 10), a glass cube-corner (a prism in the shape of the corner of a cube) fallsinside a vacuum chamber, remaining parallel to itself i.e. a pure vertical translation. A precise measurement of the change in position is performed with a Michelson interferometer, which uses laser rays. Knowing the travel time and the length of the displacement, g can be computed.

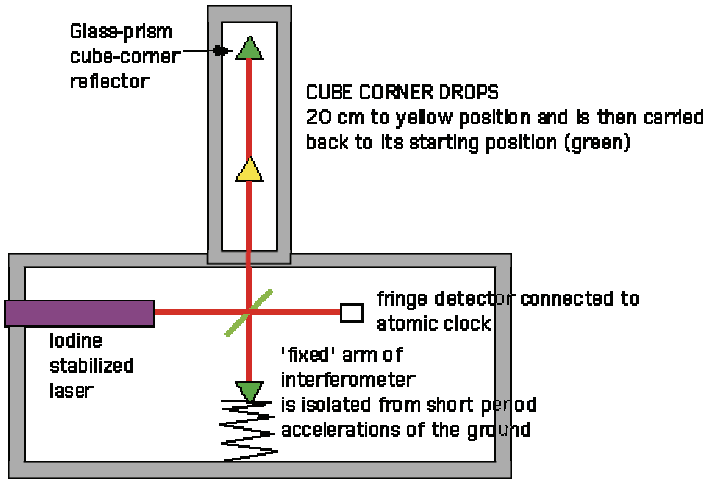

Figure 10. Scheme of an absolute gravimeter.

1.9. Field corrections with relative gravimeters

The observed g is corrected in the field for several influences:

$g_{observed} = g_{field}$ + earth tide effect + instrumental drift + Eötvös effect (for measurements at sea)

g_{field} is the value that we obtain after corrections, while the earth tide effects , instrumental drift, and the Eötvös effect are removed.

2.2.1. Earth[m3] tide effect

The earth tide effect is due to the attraction of the moon and the sun. The amplitude of the tide will

vary as a function of the position of the two bodies relative to each other. The effect is smallest when they are in opposition and largest when they are in conjunction.
The amplitude is large enough to be detected by a gravimeter. The tide depends on several factors: latitude, longitude and the time (moment of the measurement). The maximal gravity effect of the earth tide is 300 µGal or 0.3 mGal. There are different models to compute them, several reference are given in §3.4.1.

2.2.2. Eötvös[m4] correction

The Eötvös correction has to be applied whenever measurements are carried out from a ship or airplane. The earth's force of attraction is decreased by the centrifugal force of the earth. Indeed, the angular speed of a body going to the east is larger than the angular speed of a stationary body. As a result, the gravity acceleration g decreases when a vessel is going east and increases when it goes west.This is called the Eötvös effect. It is expressed as

$g_{Eötvös} = g_e = 7.503\ v \cos\lambda \cos\Phi + 0.00415\ v^2$

v is the speed in knots
Φis the azimuth of the vessel
λis the latitude

One knot is a speed of one marine mile per hour. The marine mile is an average value of a minute of latitude on a meridian arc. (1knot = 1 marine mile/hour =1.852 km/h)
Note that the Eötvös effect can have an amplitude of the same order of magnitude as the Δg signal that we are trying to measure.

2.2.3. Instrumental drift

Each gravimeter has is own life, and undergoes drift during the measurement.Computation of the drift is done by measuring the same pointtwice, first at the beginning of the loop and again at the end of the loop. After substracting the value of the earth tide the reading difference is the drift of the instrument in the interval between the measurements.

Example :
observation g_1 at the node at time t_1 (13h), and observation $g_6$at time t_6(14 h) at the same node;
observation of unknown points: g_2 at time t_2 at 13h15 etc…
If M_{tide} is the value of the Earth Tide (which changes continually in time):

$$[g_1(t_1)-M_{tide}(t_1)]-[g_6(T_6)-M_{tide}(t_6)] = \text{drift over 60 minutes.}$$

$$\Delta g \text{ between } g_1(t_1) \text{ and } g_2(t_2) = [g_2(t_2)^* (\text{drift} * 15/60) - M_{tide}(t_2)]-[g_1(t_1)-M_{tide}(t_1)]$$

This expression gives the observation at point 2 corrected for the tide and the drift.

1.10. Corrections[m5] applied at the office

The following corrections are performed to allow comparison of thedata measured at different altitudes and in different geological context.
In the following formula:

$$g_{field} = g_0 + g_{fa} + g_{bg} + g_{iso} + g_{geol}$$

g_0 is the ellipsoid attraction, g_{fa} is the free air correction, g_{bg} the Bouguer correction, g_{iso} the isostatic correction, and finally g_{geol} is the value that geologists are interested in.

2.2.4. An[m6] ellipsoidal model for the normal earth

The complexity of the density variation inside the earth explains why we must take as a reference a

spheroidal surface. There is an international agreement concerning this reference, namely a rotating spheroid with an averaged density of 5.515 g/cm³ or T/m³.

The flattening explains why the value of g at the equator and on the pole are different; it is larger by about 4 Gal at the poles. This value shows the radial variation of the earth model. In a spheroid model there is symmetry with respect to the centre and to the rotation axis.

The shape of the spheroid is that of an ellipsoid of revolution. It can be described by two parameters: the equatorial radius *a* and the polar radius *c*. It is often described by its flattening factor f :

$$f = \frac{(a-c)}{a}$$

The earth is approximately spherical with a flattening of 1/298.25. This property will allow simplification, so a section through the earth going through the poles defines an ellipse, and it can be described mathematically with a varying radius :

$r = (1 - f sin^2 \lambda)$ where λ is the latitude.

The gravity force is the vectorial sum of the attraction force due to the earth's mass and the centrifugal force generated by the earth's rotation. The gravity potential of the spheroid is the sum of the gravitational potential U_g and the centrifugal potential U_r.

$$U = U_r + U_g$$

This spheroid potential is described by four parameters: the equatorial radius a , the flattening f , the angular speed ϖ , and the mass of the earth M (Heiskanen and Moritz, 1967)

The centrifugal potential is :

$$U_r = \frac{1}{2}\varpi^2 r^2 cos^2 \lambda$$

The gravitational potential is :

$$U_g = -\frac{\gamma M}{r} - \frac{\gamma M a^2 J_2 \left(3\sin^2\lambda - 1\right)}{2r^3}$$

γ is the gravitational constant : 6.67*10^{-11} m³kg^{-1}sec^{-2}; J_2 is the dynamic flattening of the spheroid : 0.001802626 m³/s²

If the spheroid is approximately spherical any normal to the spheroid will be almost parallel to r. The normal gravity on the spheroid is :

$$g_0 = -\frac{\partial U}{\partial r}$$

And finally :

$$g_0 = g_e\left(1 + f' \sin^2\lambda\right) \text{ with } f' = \frac{g_p - g_e}{g_e}$$

f' is the gravitational flattening. The value of the parameters g_e, g_p , f' , are 9.780327 m/s², 9.832186 m/s² and 0.00530 respectively. The gravity variation between the equator and the poles is only 0.5 % but this variation is huge compared to variations caused by geological sources.

In developing this equation :

$$g_0 = g_e\left(1 + f' \sin^2\lambda\right)$$

it becomes

$$g_0 = g_e\left(1 + \alpha \sin^2\lambda + \beta \sin^2 2\lambda\right)$$

g_e equatorial attraction of the spheroid, α and β (Heiskanen & Moritz 1967) are computed with a , f , ϖ et M (defined above).

The previous equation is the truncation of an illimited series. It can be written in a more compact form:

$$g_0 = g_e\left(\frac{1 + k\sin^2\lambda}{\sqrt{1 - e^2\sin^2\lambda}}\right)$$

In this equation k and e (Heiskanen & Moritz 1967) are computed with a , f , ϖ and M . This equation is called the ***Somigliana equation*** (Italian mathematician, 1860-1955). It has been used in all the latest Belgian computations concerning gravity.

It is useful to conclude this subsection by looking at the evolution through time of the parameters of the different geodesy systems of the 20th century.

Table from Chovitz (1981)

System	a *in km*	f	J_2 (m³/sec²)	$\gamma M\left(\frac{m^3}{sec^2}\right)$	g_e
1924-30	6378.388	1/297.0	0.0010920	$3.98633\ 10^{14}$	9.780490
1967	6378.160	1/298.247	0.0010827	$3.98603\ 10^{14}$	9.780318
1980	6378.137	1/298.257	0.00108263	$3.986005\ 10^{14}$	9.780327

Three international systems have been established since the year 1930. The first system was the International gravity formula in the 1930 geodetic system.

$$g_0 = 9.78049\left(1 + 0.0052884\sin^2\lambda + 0.0000059\sin^2 2\lambda\right)$$

A new reference ellipsoid was accepted in1967, with the following International gravity formula in the 1967 geodetic system:

$$g_0 = 9.78031846\left(1 + 0.0053024\sin^2\lambda + 0.0000058\sin^2 2\lambda\right)$$

More recently a new system was accepted. It is the geodesy system 1980 which led to the 'World Geodetic System 1984'or WGS84 as it is used today, with the following gravity field reference formula, in its compact form.

$$g_0 = 9.7803267714\left(\frac{1 + 0.00193185138639\sin^2\lambda}{\sqrt{1 - 0.00669437999103\sin^2\lambda}}\right)$$

The g_0 is called the theoretical gravity or normal gravity.

2.2.5. The[m7] free air correction

This correction is based only on the height and does not depend on the mass. With this condition the equation can be written :

$$g_{(r+H)} = g_{(r)} + H\frac{\delta g_{(r)}}{\delta r} + \cdots$$

where g at the height H equalsg at H= 0 plus theδg from the height difference

We truncate and we rearrange the equation terms

$$g_{(r)} = g_{(r+h)} - h\frac{\delta g_{(r)}}{\delta r}$$

and since $g_{(r)}$ lies on a sphere,

it is $g_{(r)} = \frac{GM}{r^2}$

According to Newton's Law

$$F = \frac{GMm}{r^2} = g_{(r)}m$$

The derivative of $g_{(r)}$ is

$$\frac{\delta g_{(r)}}{\delta r} = \frac{-2g_{(r)}}{r}$$

and the expression $h\frac{-2g_{(r)}}{r}$ gives the difference of g between $g_{(r)}$ and $g_{(r+h)}$

The expression

$$g_{(r+h)} = g_{(r)} + H\frac{\delta g_{(r)}}{\delta r} + \cdots$$

becomes

$$g_{(r+h)} = g_{(r)} - H\frac{2g_{(r)}}{r}$$

When taking g and h at the averaged sea level, the free air correction becomes $g_{fa}=0.3086*10^{-5}*h$

2.2.6. The[m8] free air anomaly

$\Delta g_{fa}=g_{field}+g_{fa}-g_0$

For g_{fa} the correction is positive since g decreases when H increases. It was explained in the previous subsection that there is a linear relationship between this correction and the topography.

2.2.7. The[m9] Bouguer correction

The theoretical gravity and the free air correction do not take into account the mass between sea level and the topographical height of the measurement. We have to carry out a so-called plateau correction or Bouguer correction[2].

The Bouguer correction $g_{bg}=2\pi G\rho H$,

Where G equals 6.672×10^{-3} when g_{bg} is expressed in milligals and ρ in g/cm³. ρ is the density of the rocks between the height of the measurement and sea level. An accurate rock density above sea level is very important for this reduction. If it is poorly chosen, there is an overcorrection or an undercorrection, and the topography will be visible in the maps.

2.2.8. The[m10] simple Bouguer anomaly

The simple Bouguer anomaly is formulated as follows:

$\Delta g_{bg}=g_{field}+g_{fa}-g_0-g_{bg}$

Where g_{field} is corrected forthe earth tide effect and instrumental drift, g_{fa} is the free air correction (g corrected for the height), g_0 is the part of g related to the reference ellipsoid, and g_{bg} is the Bouguer correction attraction of the mass between sea level and the altitude of the measurement.

[2] Pierre Bouguer was a French mathematician, 1698-1758.

2.2.9. Terrain[m11] correction

Where the topography has a significant relief, local masses influence the measurements in the field.A point measured close to a hill shows too low a gravity, due to the attraction of the mass of the hill, and inversely for a valley. We have to take into account the local topography. We compute a $g_{(t)}$ which stands for $g_{(terrain)}$. We calculate the repulsive or attractive effect of the mass as a function of the distance from the measurement point.

2.2.10. The[m12] full Bouguer anomaly

The full Bouguer anomaly is defined as the simple Bouguer anomaly minus the terrain correction, or $\Delta g_{bg}=g_{field}+g_{fa}-g_0-g_{bg}-g_{(t)}$

2.2.11. Isostasy[m13] correction

Following the isostasy principle, the excess mass associated with the topographical height at the surface of the earth is compensated by a deficit of mass at depth, called isostatic root. The effect of this deficit is not taken into account in the Bouguer correction. At the scale of mountain chains, there is a close correlation between negative Bouguer gravity anomaly and positive topographical altitude. The isostatic correction supresses the gravitational effect of the isostatic roots. The depth estimates are based on the d'Airy-Heiskanen model (Simpson et al., 1986). This correction is mainly to be considered in mountainous areas. These are generally associated with negative Bouguer anomalies.

2.5. Remark[m14] on the accuracy of the measurements

An error of one mGal can be generated by a bad positioning : at a latitude of 45°, an error of 200 m causes an error of 0.5m in height. An error of 0.01m/sec (0.02 knot) in the speed of a vessel at a latitude of 45° causes an error in the azimuth (N) of 0.1 degree.

1.11. Origin[m15] of the Bouguer anomalies

The density variations of the rocks at the surface of the earth range between 1.6 and 3 T/m³. This wide range is mainly due to porosity differences of the rocks, but also to rock type. For each type of rock the density increases with the quantity of fluid present in the pores. But for most of the rocks the densities are quite close. In Belgium density is roughly correlated with the age of the rocks. In rocks of the Lower Palaeozoic, i.e. Cambrian to Silurian, density ranges from 2.7 to 2.72 T/m³. For the Upper Palaeozoic, i.e. Devonian and Carboniferous, density ranges from 2.6 to 2.65 T/m and for the Meso-Cenozoic the range is 2.1 to 2.2 T/m³. Within each group, the difference is rarely more than 0.3 T/m³. It should also be noted that density increases with depth (Strykowski, 1995)

1.12. Variations[m16] of structural origin

Structurally, rocks in a tabular setting do not show any gravity variation. In the case of a vertical fault, there is generally a gravity gradient. An intrusion of lighter material, for instance a salt dome, will give a negative anomaly. The main problem in understanding the causes of anomalies is the ambiguity between different possible solutions. To make a good interpretation, knowledge of the local geology is needed.

3. Building of a network

1.13. General[m17] organisation of a survey.

The size of the area and the required density of the observations will determine the length of the mission, knowing that on average 20 points can be measured per day. In present-day surveys with

random spread of observation points, the points are plotted in advance on topographic maps. For each point, access by road should be planned in advance, and zones of difficult access have to be identified. Woody areas will give problems for the GPS measurement. Classical levelling may be necessary, but it is time-consuming and will slow down the survey. Permitting may be necessary in big private properties or in military zones. Big industrial zones should be identified because they often generate vibrations during the day and make gravity measurements noisy. It is impossible to make measurements with a LaCoste when a truck is passing by.
It is important to inspect previous data if they exist, and check their accuracy and density. This will give an indication of the expected variation. Knowing the approximate g value will also allow to "reset the level" of the g reading of the D model in the working zone appropriate for the geographical location (see below). The measurements can have different objectives. Gravimetric prospection does not require a high level of accuracy (0.1 mGal) and optical measurement is sufficient (see below). On the other hand, microgravity and measurements for the geodesy network need very accurate measurements, a realistic accuracy being 10 µGal. The grid cell size should be smaller than the size of the body to be detected.

The field car is prepared in advance, with a special box for transportation of a LaCoste-Romberg gravimeter. The Scintrex gravimeter is attached to the back seat of the car. All instruments need to be handled with utmost care. Overnight accommodation of the operator(s) should be planned keeping in mind that the gravimeter should be kept in a safe place and under electrical tension, to keep the internal temperature around 50° C (during the day this is achieved with a battery which also needs reloading at night). A cold gravimeter does not work properly; a gravimeter that was switched off for a certain period needs twice this time to warm up again and be operational.

1.14. Field[m18] Measurements.

2.2.12. Measurement[m19] with a LaCoste-Romberggravimeter

There are two models of LaCoste-Romberg gravimeter : G and D.
The G model is called geodetic. It has a working zone of 5 Gal, which covers the whole earth. The operator reads the number of turns (including decimals) of the "nulling dial" needed to bring a mass (see below) back to equilibrium after exposing it to the local gravity. Conversion of this reading into mGal is not linear but depends on the gravity intensity. Therefore the factory provides a calibration table with 70 fictive gravity zones (latitudinal and/or altitudinal). The dial is graduated in units very close to 10 µGal. This gravimeter shows a strong drift of up to 60 µGal per day.
The D model is designed for prospection, with a working window of 200 milligal. It is equipped with a "level reset" to change the working zone and there is only one calibration factor, valid for the whole range of values within the window. The dial is graduated in units close to 1 µGal.
The two models G and D look the same, except that the reduction of the working zone in the D model decreases the possible mechanical error with a factor 10.

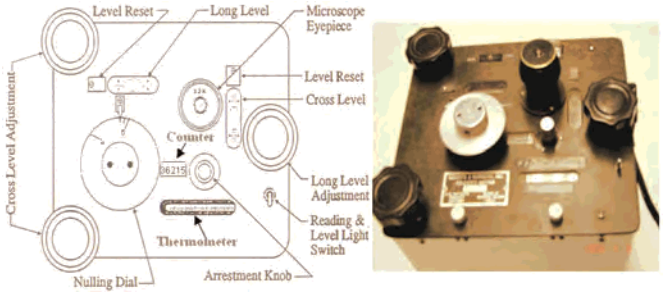

Figure 11. The LaCoste-Romberg gravimeter.

The LaCoste-Romberg has to be levelled in a strictly horizontal position before making the gravity measurement, and this is achieved with three levelling screws. Having to adjust three screws causes some mechanical problems. To reach a reading accuracy better than 10 µGal, we use the following

"earth tide" technique, developed at the ROB in 1974 (see § 4.1). The meter is fixed on a triangular base which has three legs: a fixed-height swivel with a pin in the right angle of the triangle, and two screws in the other angles, which allow the gravimeter to be levelled in two directions perpendicular to each other. The main advantage is that the height of the gravimeter is constant relative to the ground. Another advantage is the stability of the instrument. Finally there are only two levelling screws independently of each other. The name "earth tide" technique refers to the enhanced precision of the measurements, which enable earth tides to be recorded (these cause a diurnal variation of up to 300 µGal).

Figure 12.Pictures of the LaCoste without a triangular base (at left) and with a triangular base (at right), taken at the fundamental reference point of the Belgian network.

Figure 13. Gravimeters set up for field work. At left the G402 (ROB) and at right the D 32 (MGI), both fixed on a triangular base. To the right of the instrument there is a digital recorder. Above left a field notebook to help the operator to check the behaviour of the meter.

Figure 14. Instrument setup for measurement in the field. Notice the spotting nail between the instruments.

After levelling the instrument, when looking into the eyepiece one sees a graduated scale with a crosshair (or reading line) which will be eccentric at the beginning of the observation. By turning the "Nulling dial", we bring this "reading line" to a certain value which has been set by the manufacturer of the instrument, and is written on the label fixed on top of the instrument. By convention in all gravimeters we have to put the reading line slightly to the right of the given graduation (see the figure below). For a network with a desired accuracy of 1mGal we can consider this optical reading to be the final registration.

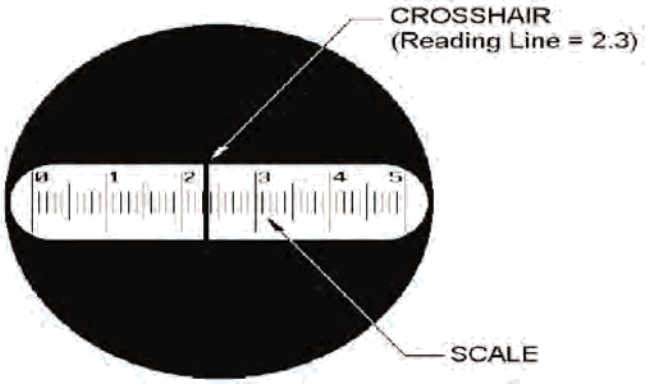

Figure 15. Reading line of a LaCoste-Romberg gravimeter.

For greater accuracy, the electronic output of the gravimeter can be used. Indeed, when the mass (beam) has been adjusted to exactly its horizontal position, the resulting voltage will be zero; generally a small disequilibrium subsists after the optical adjustment, and we measure this difference as either a voltage or a frequency proportional to the deviation of the beam from its reference position (0 volt).This electronic reading is identical to the microscope reading but is not biased by an observerand is more accurate. With this method we can interpolate to the µGal. High-frequency seismic noise, of the type caused by road traffic, is rejected by a microseismic filter before being transmitted to the electronic reader. Electronic reading only (without the optical reading) has another advantage, in that it avoids thermic perturbation by the lamp.

A measurement is made in the following sequence. Adjust the reading line with the Nulling dial to the necessary value (according to the manufacturer), which brings the voltmeter to 0 Volt. Then turn the Nulling dial first until +100 µGal, read the voltage, then until -100 µGal, read the voltage again (this calibrates the instrument and stabilises it after each transport), get back to 0 Volt, then do the same at

+10 µGal and -10µGal, and finally get back to 0 volt. We can now interpolate the Voltage value corresponding to 1 µGal, and obtain the true value of g. This procedure is also helpful to detect operator mistakes.

2.2.13. Measurement[m20] with Scintrex CG3M and CG5 gravimeters

This gravimeter is user-friendly for the operator. The first advantage is that this gravimeter is geodetic, meaning that it can be used on the whole earth like the G model of LaCoste. The reading resolution is 1 µGal and the standard deviation is less than 5 µGal. Levelling is made with three levelling screws. There is a unique calibration factor that can be easily calibrated with a tie between two absolute points.The operator is in front of the electronics device. The correction and filters(tide correction, continuous tilt correction, auto reject, terrain correction, seismic filter, raw data to save or not) must be fixed before the field measurement. The instrument reading option has also to be fixed. The instrument records the readings in its internal memory. After a day's work the operator downloads the readings on a pc. With the appropriate software, the operator can directly reduce the data in the field and it can quickly be checked if some loops have to be measured again. On the CG3Mgravimeter (fig. 16), the measurements are directly accessible in digital form. In the first lines of the file all measuring parameters are noted.

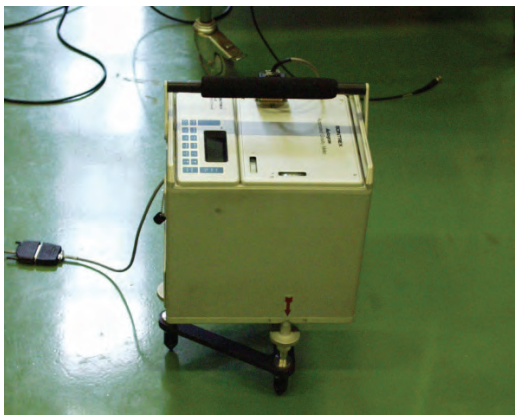

Figure 16. The Scintrex CG3M Gravimeter.

The CG5(fig. 17) is based on the same concept. It is slightly smaller and the interface is even more user-friendly. Results can be downloaded through a RS232 or a USB connection. Unfortunately to download the data a special Scintrex software (SCTUTIL), delivered with the instrument, is needed.

Figure 17. The Scintrex CG5 gravimeter, with a zoom-in on the interface; the reading is in mGal.

1.15. Setting[m21] up the network

Setting up the survey network requires selecting the locations of the measurements. A maximum number of existing levelling benchmarks, known with X, Y, Z coordinates, are used. The other points are then positioned on the map in a homogeneous grid with regular random spacing but not in any geometrical grid. Measurements are performed in a certain sequence defining a loop, where the node is defined as the point of departure and return of the loop. At least one point of the loop should be in common with another loop, and ideally each loop should have at least one benchmark. We tie the network to a maximum number of first-order gravity points, generally lying outside the network to be measured. By integrating first-order gravity points in the network, all surveys are ultimately tied to the reference point of Uccle. Each day the loops of the day are laid out, taking into account the weather forecast and local traffic conditions. Nodes are marked in the field with a spotting nail (fig. 18), to facilitate a later check or a later continuation of the survey; nodes are therefore better selected on a road, a concrete slab or other man-made substratum (compare fig. 14).

Figure 18. Spotting nail

The advantages of this method are :

1 Adaptation to the field conditions

2 Possibility to progressively adjust the network and to find errors in the loop.

3 At all times the network can be interrupted and continued, even after a few years, if the nodes can still be located and are well-preserved.

For the first gravimetric networks(until 1996) the height was measured with a theodolite. However this required a second field team; height was determined with an accuracy of 1 cm/km, and the advancement was 6 km/day. For the altimetry, the reference for Belgium is also located at the ROB: it is exactly 100,174 m and it was fixed by the first-order levelling network in 1840-1879.
In this case, points are first plotted on a map, their position is digitised with a reading error of ± 2 mm, which means ± 20 m on a map of 1/10000, which in turn means ± 16 µGal of latitude effect (or ± 50 m at the scale 1/25000, which means ± 40 µGal).

At present with GPS location, latitude φ and longitude λ are known to the centimetric level.GPS determines the X, Y, Z coordinates, but the altitude measurement requires reprocessing of the data to obtain a maximum error of ± 2cm. We have to keep in mind that an altitude error of 1 cm represents a gravity error of 3 µGal. It is one of the reasons for the use of the triangular base plate under the LaCoste gravimeter. When using the Scintrex, only two of the three levelling screws are used, to have a constant distance to the ground. In levelling a benchmark, its height is brought to the ground level.

The existence of permanent GPS networks, built and maintained by the regions (Walcors in Wallonia and Flepos in Flanders) and checked for consistency by the National Geographical Institute, together with the availability of Differential GPS devices (DGPS), and the existing detailed gravity geoid HBG003, have greatly improved the speed and the quality of gravity acquisition in recent years. Indeed, once the equipment has been taken out of the field car, the levelling can now be achieved in about three minutes, and the gravity reading in another ten minutes. In turn, these new gravity observations will contribute to a better accuracy of the geoid, especially in regions with higher relief.

1.16. Processing[m22] of the gravity data

Processing is done by different types of software, and itneeds to be done by an experienced person who can check which data to keep or to reject.

2.2.14. Reduction[m23] of the measurement

Reduction of the data means to transform the reading taken in the field into Δg, applying different corrections.
At each measurement station we estimate the sensitivity of the electronics of the LaCoste-Romberg instrument by making measurements of the + 100 µGal and – 100 µGal values (see above). The average between the zero, + 10 µGal, - 10 µGal voltage readings are used to compute the g value of the point in µGal, using the calibration table.
This long procedure has some additional advantages:

- The 10 minutes needed to stabilise the mechanical part of the instrument are used in a useful manner to determine a conversion from voltage to counter units.
- The successive readings are used to check the stability of the instrument and to detect bad measurements, reject them if necessary and repeat them.

For the Scintrex we average 5 or 6 discrete measurements in each point. As for the LaCoste, bad data are eliminated by statistical criteria. Readings on the gravimeter are transformed into µGal with a calibration factor, which is generally close to one for the Scintrex.

Earth tide correction is made in two steps: the calculated earth tide factors, valid for a whole regional survey, are applied to a potential. The earth tide factors (Melchior, 1971, see § 4.1) are calculated for a point situated in the centre of the network. They are based on a model of solid earth, this is an elastic earth without oceans and with a liquid core (Molodenski model, Molodenski, 1967). The indirect effects due to the interaction between oceanic tides and the crust, are calculated with 8 cotidal maps (oceanic tide maps from Swiderski, 1980). An error of 5 cm in the amplitude of the tides results in an error of 0.5 µGal. The potential of Cartwight-Taylor-Edden (Cartwright & Edden, 1967), accurate to 1µGal, is used with the earth tide factors, to obtain the correction for each point.

At the end of each loop the averaged value of each station is corrected for the instrumental drift (the difference between two measurements on the same node) by a linear interpolation model. After the removal of the drift correction we obtain Δg between the stations.

2.2.15. Adjustment[m24] of the networks

From this reduced file, we retrieve the ties between the nodes, the nodes being the points where more than one measure was carried out at different times in the network, and the ties being the calculated Δg between two nodes. We make a “free adjustment of the network” by least square adjustment of the nodes. We obtain for each node an adjusted value and its residue. This gives an idea of the quality of the network. We can check the scale of the instrument using measurements in known points. We then distribute the residue over the intermediate observations, and we can have an estimate of the error in each station.
To obtain the real g value we start with a station with a known g (first-ordergravity point) and then the whole network is referenced to Uccle.

1.17. Potential[m25] error sources in the gravity data

An error can be linked to:
- the coordinates being expressed with respect to different ellipsoids. Belgian data are defined relative to the Hayford ellipsoid.
- the altimetric datum. In Belgium there is a difference in altitude of +2.32m compared to the REUN (Réseau Européen Unifié de Nivellement).
- to a bad positioning in x, y or of the altitude H.
- to a wrong gravity reference; the Belgian reference is in Uccle (Brussels) and is equal to IGSN71-0.048 μGal, where IGSN71 is the worldwide reference (Morelli, 1971, see § 4.1).

4. History of gravity measurements and maps in Belgium.

1.18. History[m26] of gravity measurements

This historical overview aims at describing the important steps leading to the present-day complete gravity coverage of Belgium. We will not talk about local measurements made in Belgian laboratories for metrological purposes, but focus on those measurements that contribute to understanding the spatial variation of gravity over the extension of the national territory. These allow an interpretation to be done in terms of underlying geology, and also furnish the highest possible precision for geodesy work such as the calculation of the geoid. This section will also give some biographical notes on scientists who contributed to the field gravity networks at the national scale.

1892
Delforges from the “Service géographique” of the French army realises the first gravity measurement in Belgium. It is performed at the Royal Observatory of Belgium (ROB) in the room called the “Salle voûtée” , using a pendulum. The recorded measure is g=981 169 mGal, based on the g defined in Paris as g=981 000 mGal .

1897
Acquisition by the Belgian Antarctic expedition (under the command of de Gerlache) of an instrument called Von Sterneck (3 pendulums made of brass, gold coloured, fabrication numbers 104, 105, 106). With this instrument (fig.19), Danco realises measurements:
- in the Geographical Institute in Vienna under the direction of Von Sterneck.
- in Uccle at the Royal Observatory of Belgium in the old anemometer house (this house is later destroyed in 1908). The measurement is g=957 635 mGal, and this is obviously false, because the value of g varies only 4 Gal on the earth’s surface.
- in Rio de Janeiro.

1899
On the way back from the Antarctic expedition, after the death of Danco, G. Lecointe, scientific director of the Astronomical Service of the Royal Observatory ofBelgium and second-in-command of the expedition, makes some measurements in Punta Arenas along the Strait of Magellan. The Von Sterneck instrument was given to the Royal Military Academy in 1906; the pendulum n°105 disappeared.

1900
Helmert proposes to the International Association of Geodesy (IAG) to reduce all observations to one Unique System : the Vienna system determined by Von Sterneck.

1909
Kuhen and Furtwaengler define the Potsdam system with an absolute measurement, using a pendulum (all pendulum measurements are absolute).
Borass carries out a correction of -57 mGal to put the value of Uccle in the Potsdam system.

Result: g= 981 112 mGal at Uccle.

1921
Ch. François, a volunteer researcher at the Royal Observatory of Belgium (ROB), builds the first gravity network with the Von Sterneck instrument with four pendulums in Invar (series numbers 96,97,98,99). This instrument is now held at the ROB museum.

Biographical note: **Ch. François.**He was the pioneer of field gravity measurements in Belgium, as a mathematician with the title of corresponding astronomer (astronome correspondant) of the Observatory in Uccle. From 1921 to 1928 he used a Von Sterneck instrument belonging of the observatory, yielding the first gravity measurements in Belgium. It was very difficult at that time to make correct measurements in the field. Pendulum measurements were usually realised in an observatory where a time service was available (necessary for pendulum calculations). This is not the case in the open country. François built an astronomical clock for this purpose, and he was able to receive on long-wavelength radio the emission of the time signal by the Eiffel Tower in France.

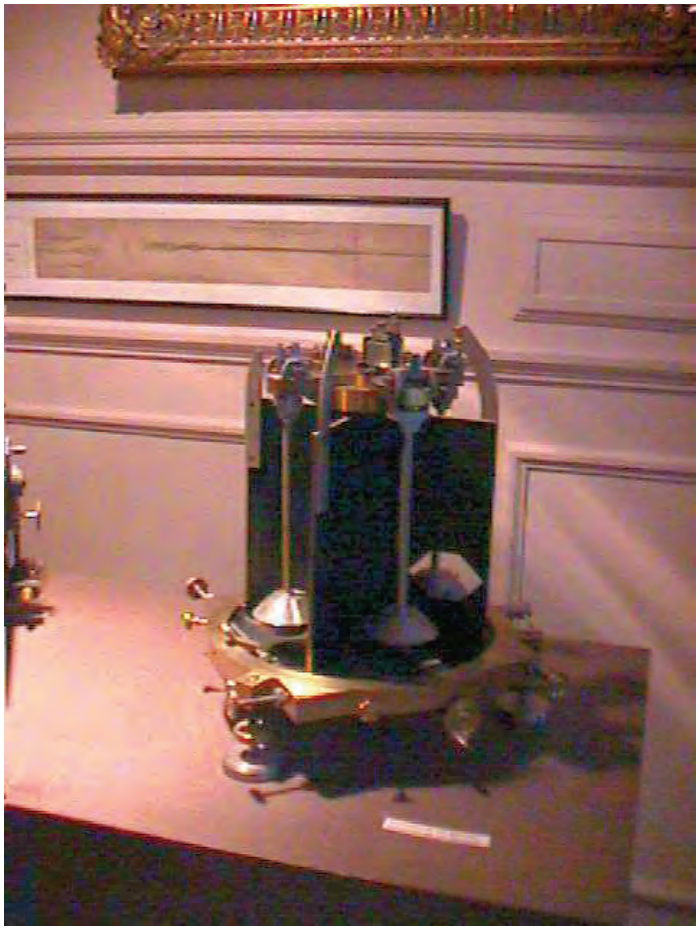

Figure 19.The Von Sterneck instrument used by Ch. François (1921).

1925
Vening Meinesz includes Uccle (as a gravimetric reference point) in the Potsdam system by connecting it through De Bilt in the Netherlands. Result: g= 981 131mGal at Uccle.

1928
Ch. François completes the first Belgian gravimetric network with 24 stations, with an error of ±1 to 3 mGal. This is the first network of the first order.

1929
Ch. François measures g at Brussels University (Université Libre de Bruxelles, ULB).

1946
Joint acquisition of a Norgaard 256 gravimeter, obtained from the National Fund for Scientific Research, by the following partners:
- The Royal Observatory of Belgium (ROB)
- The Free University of Brussels (ULB)
- The Military Geographical Institute (MGI, now National Geographical Institute, NGI)
- The Royal Metrological Institute
- The University of Liège

This gravimeter is now in the ROB museum (figure 20).

Figure 20. Two views of the Norgaard 256 gravimeter, acquired in 1946.

1947-1948
- With the Norgaard 256, L. Jones from the MGI realises the second Belgian gravimetric network. 381 stations were measured, with 25 base stations (error ± 0.35 to 069 mGal)
- He also ties the Belgian network to France and the Netherlands.

Biographical note :**Louis Jones (1914-1975)** started his military career as an officer in the artillery. After the second world war in 1945 he served at the Military Geographical Institute (MGI), where he worked as an engineer with a scientific mission. He became head of the levelling and gravity service, which grew out to be his life project. He had first to rebuild the whole levelling network destroyed during the war, and for gravity only the measurements carried out by Ch. François subsisted. The gravity map published by Jones in 1948 was one of the first maps to cover the complete territory of a

country. From 1966 he started to increase the density of the gravity measurements, adding more than 6000 points to the network, but his early death would not allow him to see the completion of his work, especially for the Flanders anomaly. He also worked in the Belgian Congo, with missions in 1952 and 1953 for the Institute of Research in Central Africa and the syndicate for mining and geological studies (Syndicat pour l'Etude Géologique et Minière de la Cuvette Congolaise). He also used gravity as a geophysical tool in civil engineering works to detect underground cavities when constructing buildings or highways. He was preparing a study on soil motions in Belgium, when he suddenly passed away in 1975.

1948
Tie of the Belgian network to the Luxembourg network.

1951
L. Jones publishes the first map of the isostatic anomalies of Belgium (Jones, 1951).

1953
MGI carries out measurements with a North American gravimeter in the eastern part of the Campine (Kempen) for the Geological Survey of Belgium. This campaign covers approximately 1500 km² with 1451 stations. Unfortunately these data have been lost.

1960
241 stations are measured in the western part of the Mons Basin by the Faculté Polytechnique de Mons, with a Worden 194 gravimeter.
Also in 1960, the Belgian Shell S.A, in collaboration with the Bataafse Internationale Petroleum Maatschappij N.V., start a campaign with a Worden 399 gravimeter, in the Dinant basin , the area of Namur-Wépion and the area of Rochefort-Serpont. This network is completed in March 1962; there are 2982 stations, among them 42 base stations.

1961
A new gravity campaign starts in Flanders by the MGI with a Worden gravimeter, to cover in greater detail the negative anomaly discovered by the 1947 survey. These data are collected over a ten-year period (see below, 1972). The measurements are the basis for following networks.
Two small studies are realised in the Mons and Battice areas.

1962
The «Société Campinoise de Recherche et d'Exploitation Minérale» (SCREM) and PETROFINA S.A., ask the MGI to carry out a gravity survey in an area of 1450 km² between Antwerp in the west, Turnhout in the east, the country border in the north, and the Albert canal in the south. This survey is measured with an Askania GS11; there are 575 stations, among them 219 base stations.

1967
The general assembly of the IAG (International Association of Geodesy) in Luzern decides to apply a **-14 mGal correction to the Potsdam system.** The value of g in Uccle thus becomes 981 117 mgal. This correction is historically very important: data from before and after 1967 should not be confounded.
The ROB defines a calibration line of 11 mGal (between the lowest and the highest point) on the Butte du Lion of Waterloo. Between 1967 and 1974, 2 North American gravimeters, 1 AskaniaGS11, 2Worden and 3 LaCoste-Romberg G (G= geodynamic model with 4 Gal scale) were used to make this calibration. Once the calibration is made, any new gravimeter can be calibrated on this hill.

1971
At its 15th general assembly in Moscow in 1971, the International Association of Geodesy (IAG) takes the 1854 stations of the IGSN71 Network as the reference for the world network. This reference is still valid in 2011. Uccle is one of the reference stations, with a recognised g value of g=981 117.32 (precision ±.032 mGal).

The I.G.S.N.71(The International Gravity Standardization Net 1971) (Morelli, 1974) is a worldwide network, consisting of 24000 gravimeter measurements, 1200 pendulum measurements and 10 absolute measurements collected over a twenty-year period and adjusted by a small Working Group. The concept differs from that of earlier gravity reference systems in that the datum is determined not by an adopted value at a single station, but by the gravity values for 1854 stations obtained from a single least squares adjustment of absolute, pendulum and gravimeter data. The I.G.S.N.71 point for Belgium is situated in the gravimetric cellar in the Royal Observatory of Belgium and marked by two nameplates on both sides of the fundamental pillar.

Still in 1971, M. Coen from the UCL (Université Catholique de Louvain) builds a detailed network of 226 stations for a gravimetric prospection of the Han caves massif.
- P. Melchior publishes the first treatise on gravimetry in Belgium (Melchior, 1971)
- The Compagnie Générale de Géophysique (CGG) performs a detailed survey commissioned by the Geotechnical Institute of the State, along the trace of the Brussels-Paris highway south of Nivelles, to detect underground cavities, with 6161 stations. This survey was completed in 1972, but unfortunately the data has not been kept.

1972
For internal reasons, the MGI discontinues the network measurements started in 1962 in the north-east of Belgium. In total 6280 stations were measured in the fundamental framework of 1947-1948.

1974
The ROB develops, together with the International Latitude Observatory of Misuzawa (Japan), a technique to increase the resolution of reading measurements of LaCoste gravimeters. This technique enables reaching a reading precision of a few microgals (see below).

1975
The gravimetric cellar of the University of Louvain-la-Neuve is linked to the Belgian network and to IGSN71.

1976
The University of Hannover (Germany) measures 8 Belgian stations within the North-West European Lowland Levelling Network (NWELL).
First absolute measurement in Belgium in the gravimetric cellar of the ROB, carried out by the Instituto di Metrologia and the Instituto di Miniera e Geofisica Applicata dell'Universitá di Trieste (Cannizzo et al., 1978). Result: g= 981 117.301 mGal.
The CGG measures a detailed network in the area of Charleroi, with 6877 stations, started in 1975, on behalf of the Geotechnical Institute of the State, to determine the best geological structures to bury water pipes. Unfortunately the data has not been kept.
A detailed gravimetric survey is carried out in the area of Redu by the Technische Hochschule Darmstadt, Institut für Physikalische Geodäsie. The data has not been kept.
The NGI (National Geographic Institute) carries out gravimetric measurements with a Worden gravimeter along the 1st et 2nd national levelling networks. This work is finished in 1977, with a total of 1126 stations measured.

1977
The NGI carries out a survey of 396 stations with the Worden gravimeter in the Hamoir area (topographical map sheet 49). This data has been kept.

1978
The NGI, the ROB in collaboration with the metrological service, the UCL and the ULg (University of Liège) realise a new first-order gravity network with five gravimeters LaCoste-Romberg (n°3G, 336G, 434G, 487G, 31D). There are 36 stations in Belgium and 2 in Luxemburg. The accuracy is 0.005/0.01 mGals.

The earth tide correction is calculated, with an accuracy of one microgal, using formulae which were developed internationally (see Melchior, 1971). This calculation is from now on performed routinely in the office.

1979
The German company Prakla-Seismos GmbH carries out a survey of 481 stations over the Visé – Puth anomaly around Maastricht at the request of Martin Bless: 170 stations are in Belgium, 200 in the Netherlands and 111 in Germany. Unfortunately the data has not been kept in Belgium; they have been kept in Germany however (Skiba, 2011).

1980
From 1979 to 1980, NGI builds a complementary first-order network with the LaCoste-Romberg n°32D gravimeter. It is a network of 50 stations, the purpose of which is to connect all previous networks into a common reference frame, also available for connecting future networks.

1985
The Compagnie Générale de Géophysique (CGG) carries out for Electrobel a network of 3000 measurements in the area of Diksmuide. Thanks to the first-order network, this floating network will be connected to the IGSN 71.

1986
Start of the systematic survey of the whole country at the initiative of the Geological Survey of Belgium (GSB).Ch. Poitevin of the ROB establishes a long-lasting collaboration between the National Geographic Institute (NGI)and the ROB for the acquisition of gravity data. In the 1986 project commissioned by the GSB, 1 point/km² is measured in the area of the Flanders anomaly, centered on Ardooie.This network has 593 stations.

Biographical note: **Christian Poitevin (1951-2003)** started his career as a physicist at the National Geographical Institute NGI. He encouraged the NGI to purchase a LaCoste-Romberg gravimeter (the D32). In 1978 he participated in a new first-order gravity network. He also contributed in 1979 to realising the first acquisition system for gravity, including temperature corrections etc. In 1979-1980 he realised a complementary first-order gravimetric network (50 stations). The purpose of this network was to homogenise the pre-existing scattered surveys. In 1980 he started to work for the Royal Observatory of Belgium (ROB). For many years he participated in the installation of earth tide recording stations all over the world. 1986 marks the start of the systematic measurements of gravity under the impulse of the Geological Survey of Belgium. The NGI carries out the measurements in the field while Poitevin performs the follow-up of the different campaigns. In 1995 Poitevin left the Observatory.

1987
Measurement of 1 point/km² in a network centered on Bree in the northeast of the Kempen (Campine), on the western edge of the Roer Valley (Roermond) graben. This is again a project of the Geological Survey carried out by the NGI and the ROB. There are 590 stations.

1991-92
Another project executed by the NGI and the ROB, as a result of the regionalisation on 1989 this time for the Flemish Region, with scientific follow-up by the Geological Survey. Measurement of 1 point/km² of the area of the Flanders anomaly, centered on Oudenaarde. There are 802 stations in this network.

1992-93
The NGI and the ROB measure two networks centered on Geraardsbergen, for the Flemish Region with scientific follow-up by the Geological Survey. There are 636 and 652 stations in these networks (1 point per km²).

1994-95
Again, for the Flemish Region, the NGI and the ROB measure a network centered on Zonnebeke located in West Flanders. There are 476 stations (1point/km²) in this network.

1995
The NGI and the ROB measure a network in the Brussels Region, commissioned by the Brussels Region. There are 415 stations, in a high-density network of 2.5 points/km².

1996
For the Flemish Region, with scientific follow-up by the GSB, the NGI and the ROB execute a survey centered on Eeklo. It is a lower-density network of 403 stations (1point/5km²).

1996
For the Geological Survey of Belgium, the British Geological Survey measures a gravimetric network limited in the west by a north-south line through Nivelles and in the east by aN-S line near Namur; it also extends from Leuven to Dinant. There are 2973 stations (1 point/km²)in this network.

1996
The ROB buys its own absolute gravimeter, a FG5 from Micro-g Solutions Inc. This Instrument enables measurement of the gravity with an accuracy of 2 µgal. The FG5 operates by using the free-fall method. An object is dropped inside a vacuum chamber (called the dropping chamber). The descent of the freely-falling object is monitored very accurately using a laser interferometer. By accurately measuring the distance covered by the corner cube, and the interval of timeto cover this distance, the value of g can be determined .

Figure 21 The FG5 of ROB.

1997
LCT Inc. carries out a gravity survey at sea on the whole continental self, for the Geological Survey of Belgium. They use an Air/Sea S-90 LaCoste-Romberg gravimeter equipped with a Zero Length Spring (ZLS).The gravimeter was placed on board of the Belgian scientific vessel Belgica. The measurements were made continuously along navigation lines parallel to one another and roughly parallel to the coast; in total 39114 points were recorded.

1998-2001
The ROB and the NGI build the third first-order gravimetric network, called BLGBN98 (the BeLGian Base Network 1998) (Everaerts et. al., 2001). This network has 41 base stations and is calibrated with 8 absolute points. The measurements were performed with nine gravimeters: seven LaCoste-Romberg models D and G, and two Scintrex CG3. The aim was to constrain the network by a scale factor by the

use of 8 absolute points. In 1978 there had been only one absolute point. In order to reach an accuracy of 0.004 to 0.01 mGal, some points from abroad were also used (e.g. Zundert in the Netherlands). A total of 60 points were measured, and 1050 tie-lines were established.

1998
For the Geological Survey of Belgium, the company Geophysik GGD from Leipzig performs a survey in two parts, first an east-west area from Dendermonde to Hasselt over a north-south extension of one topographic map sheet (20 km), and second an adjacent north-south area extending to Andenne on the Meuse, 24 km wide or one-and-a-half topographic map sheets. Gravimeters of the following types were used: LCR G503, G865, G885, and G890. There are 3205 stations (1 station/km²) in this survey.

1998
For the Walloon Region, the NGI and the ROB execute a survey of the Haute Ardenne area, in the southeastern part of Belgium and centeredon Stavelot. The network consists of 745 stations (1point/5km²).

1999
Again for the Walloon Region, the NGI and the ROB carry out a surveyin the south of Belgium centered on Neufchâteau. This network is composed of 784 stations (1point/5km²).

1999
The Meetkundige Dienst of the Dutch Rijkswaterstaat covers the northern Kempen (Campine) with gravity measurements. Due to the geographical shape of the Netherlands, especially in the Maastricht area, the Netherlands need Belgian data to calculate their geoid. As the existing Kempen network surveyed in 1962 for PETROFINA was distorted and unusable, the Netherlands decided to execute a new survey on Belgian territory. There was an agreement to exchange these data with the ROB in Belgium. This campaign covers an area of 2800 km² with 1point/5km². In total there are 441 data points.

2000
For the Walloon Region the NGI and the ROB execute two surveys, one in the Waremme area and one in the Philippeville area. The two surveys have respectively 248 and 439 stations (1 point/5km²).

2001
The company Geophysik GGD from Leipzig carries out a survey north of Liège for the Geological Survey of Belgium, with the gravimeters LCR G548 et G890. This network comprises 1201 stations (1 station/km²)

2002
The company Geophysik GGD from Leipzig carries out a survey for the Geological Survey of Belgium, located between Hasselt and the Dutch border. LCR G548 and G890 gravimeters are used. This network has 1160 stations (1 station/km²).
Also in 2002, the Flemish Region commissions a survey carried out by FUGRO, in two parts: one part in West-Flanders with 2206 stations, and the other in the Antwerp Kempen (Campine) with 1098 stations.

1.19. Historical[m27] overview of gravity maps in Belgium

All maps presented here are calculated with a Bouguer reduction density of 2.67 (averaged density for the crust), and all are referenced to Uccle in the IGSN71 system. The location of geographical features mentioned in the text (cities, regions, structural features) is indicated in figure 35 at the end of the volume.

2.2.16. First[m28] gravity map by Ch. François in 1928

This map, based on only 28 points, was published in the Annales of the Royal Observatory of Belgium (3ème série, tome I and II) (figure 22). The map already shows the main features due to geological structures. We recognise the Brabant Massif with high-density rocks in the north, and the Ardennes with Devono-Carboniferous lower-density rocks in the south. In the western part of Flanders some points with a lower gravity signal than in the east can be observed.

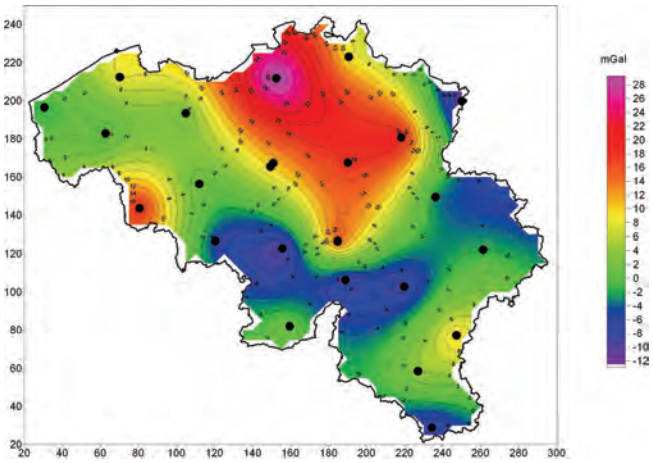

Figure 22. Bouguer anomaly map based on 28 points measured by Ch. François (1928), redrawn and coloured for the present publication[m29].

2.2.17. Second[m30] gravity map by Jones (1947-1948)

The map by L. Jones (1948) is based on 381 points (fig. 23). It was published by the Military Geographical Institute with a booklet entitled " Le levé gravimétrique de la Belgique 1947-1948". This map is a significant step forward in the understanding of the Belgian underground. On this map we see the extension of the Brabant Massif in greater detail. A steep gradient to the north-east of the Campine corresponds to the edge of the Rhine Graben. In the Ardennes we clearly see the negative anomalies linked to the Devono-Carboniferous. There is also a negative anomaly centered on Eupen. But the main new feature pointed out by this map is the strong negative anomaly in the western Brabant Massif. We also notice a gradient between the north and the south.

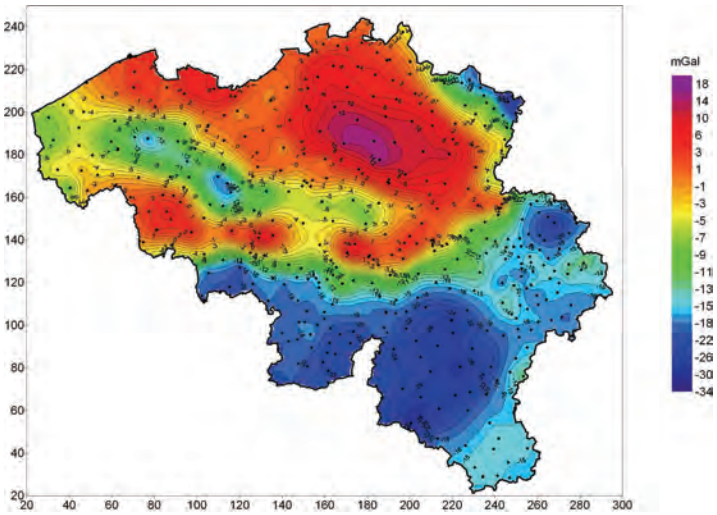

Figure 23. Bouguer anomaly map of L. Jones (1948) based on 381 points (1 point/80 km²), redrawn and coloured for the present publication.

2.2.18. Updated[m31] Bouguer anomaly map with reduction density of 2.67

In the period of accelerated acquisition of gravity data, from 1986 to 2003, the Bouguer anomaly map of Belgium was updated several times for internal use, but it was not formally published. A simplified version was published at a scale of 1: 2 000 000 by Mansy et al. (1999) with more detail in the areas where the acquisition was most advanced. This will be discussed in chapter 6.
Figure 24 below is based on the total database of gravity stations in Belgium, which was available in 2003 and has not been expanded since. It was calculated with a uniform reduction density of 2.67g/cm³.
The map was made with 30000 measurement points on the Belgian onshore territory and more than 38000 offshore (station locations in fig.27). The data from the surrounding countries have been also integrated. With such a dense network many details can be observed. The Flanders anomalies are more complex than in the 1948 map. The edge of the Rhine Graben (gravity low) can be followed rather closely. The Brabant Massif extends further to the north. We also see a sharp gradient marking the limit between the Brabant Massif and the Ardennes region. This corresponds to the concept of the "Faille Bordière" or border fault (Legrand, 1968) although it does not perfectly coincide with it at the outcrop level. This sharp gravity gradient is located just south of the Sambre and Meuse valleys, and is oriented west to east in the western part, and south-west to north-east in the eastern part, with an elbow near Huy. It is sharper near Liège in the east, and also especially to the north of the Mons Basin, where it is locally enhanced by the lighter sedimentary material in the Mons Basin. In the Ardennes there is an negative anomaly centered on Eupen, and a very wide anomaly in the Synclinorium of Dinant, extended towards the Givonne inlier. A positive anomaly occurs along the Neufchâteau – Eifel anticline.

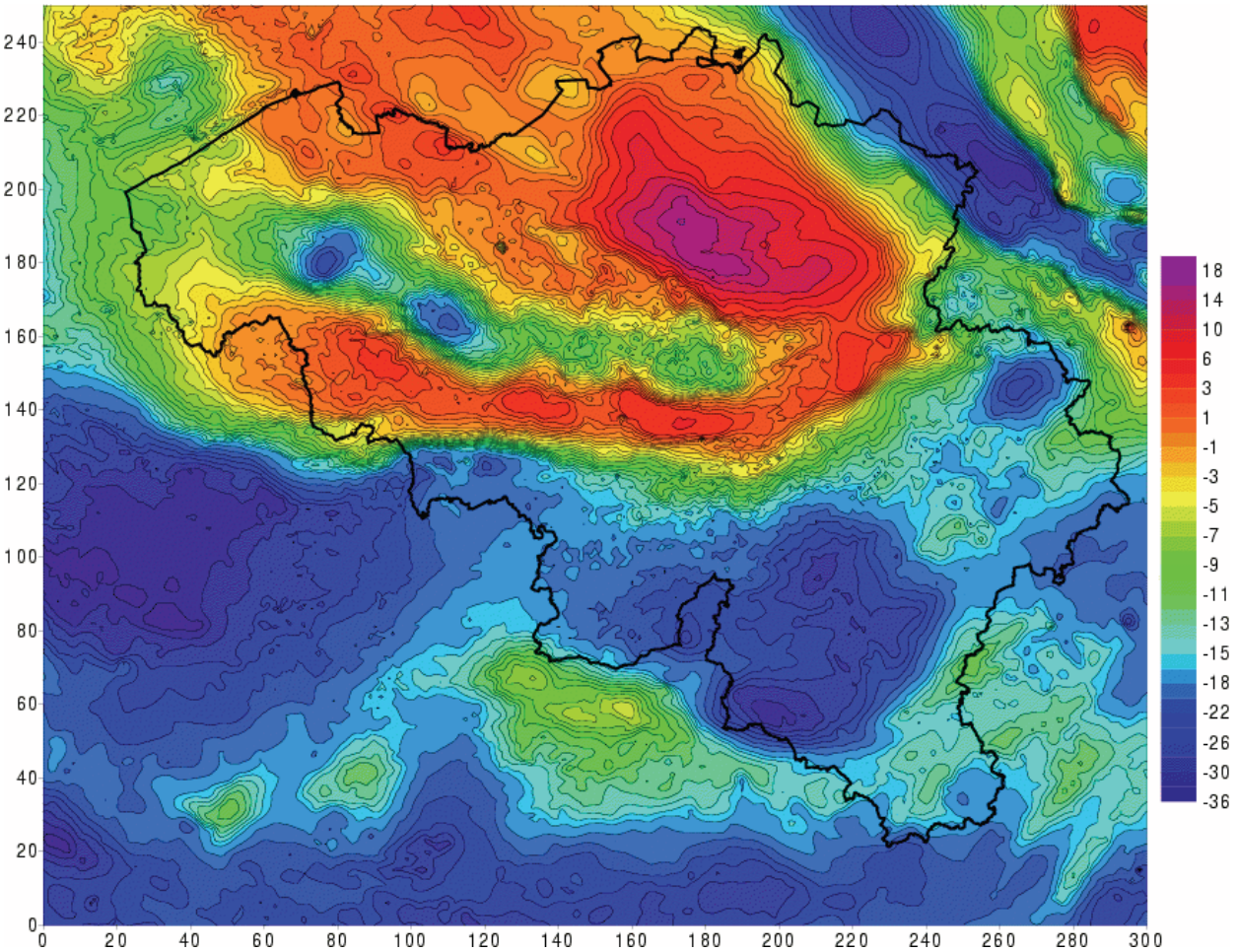

Figure 24. Up-to-date Bouguer anomaly map of Belgium calculated with a reduction density of 2.67. over all the Belgian territory (2011, this work).

2.2.19. The[m32] free air anomaly map

The free air anomaly map is the basis for the calculation of the Geoid, as explained in the chapter on the calculation of the anomalies (chapter 3 below). In order to calculate the free air anomaly, from the g value measured in the field we subtract the $g_0$which is the theoretical g value for the location according to the ellipsoid WGS84, and we correct also for the altitude, to reduce the value to sea level.

The free air anomaly map (fig.25) shows many features from the topographic map because no correction is performed for the mass present between the measurement point and sea level.
In the Ardennes we recognise the high altitude plateau and more specifically the Hautes Fagnes – Venn-Eifel area in the east. The valleys in the Ardennes are visible, most conspicuously the Meuse valley. In the north however, as relief in less pronounced, we do not see altimetry but deep-seated geology. We clearly see the negative Flanders anomaly due to a mass deficit, and a positive anomaly in the Diest area. The Rhine Graben is also apparent.

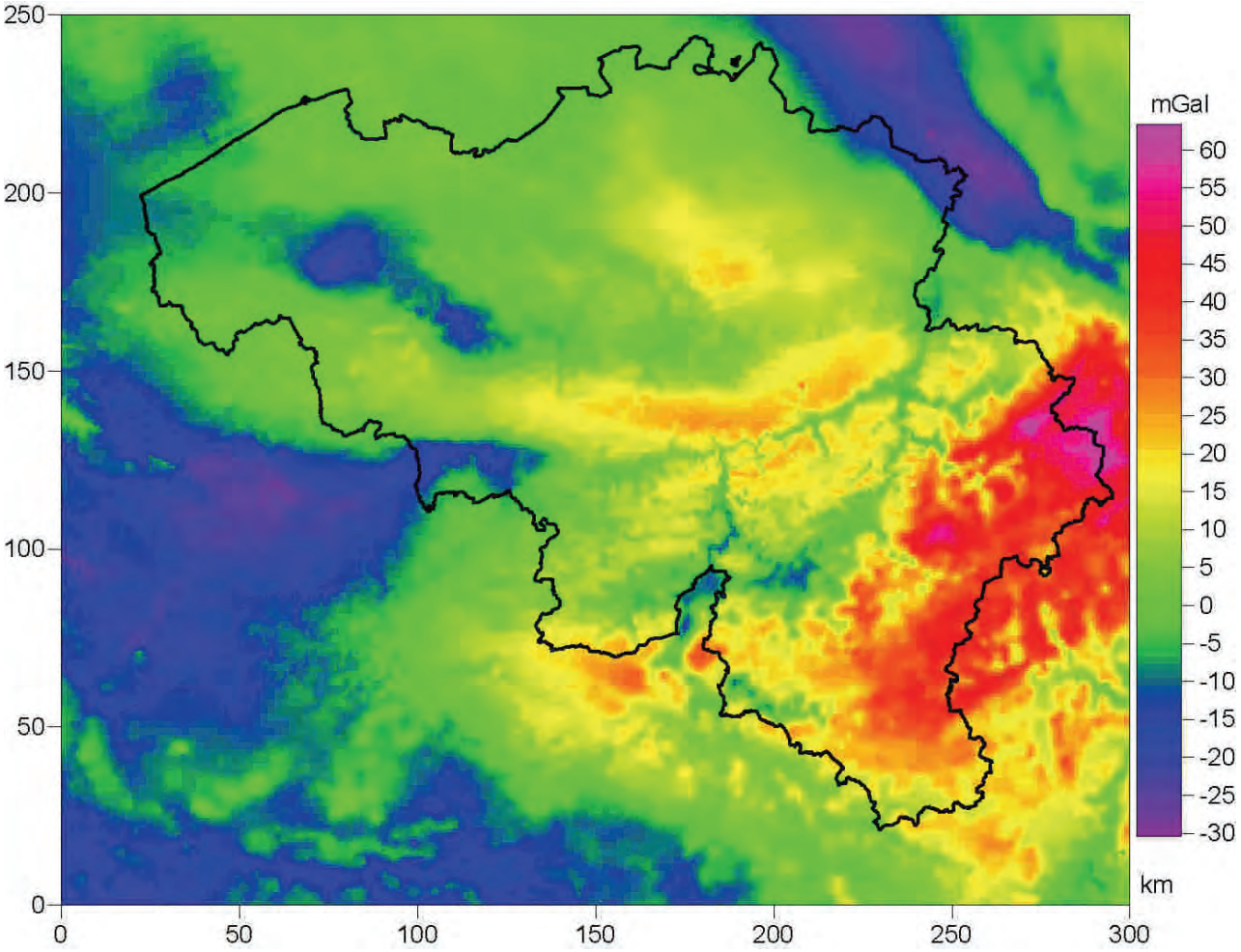

Figure 25. Free air anomaly map of Belgium (2011, this work).

2.2.20. The[m33] map of g

This map represents the field measurements. The only corrections applied to these data are the so-called diurnal corrections, i.e. temporal variations during the day: the earth tide correction and the instrumental drift.

As we know, the principal causes of the gravity variation at the scale of the earth are latitude and altitude. The earth is flattened at the poles, with a flattening of 1/298.25. The polar radius is shorter than the equatorial radius.As the equatorial surface lies farther away from the center of the earth, the

value of g at the equator is smaller than at the pole. This phenomenon is clearly visible even at the scale of Belgium (fig. 26). There is a north-south effect of 0.3 Gal (cm/s²) or 300 mGal on our territory. Geology also influences the value of g sufficiently to perturb the equipotential curves of g, which deviate from the expected east-west orientation. For instance, near the Rhine Graben where thick lighter sediments of Meso-Cenozoic age are present, g is lower than at the same latitude to the west and east.
The second effect is due to the altitude. Areas with high altitude appear to weaken the latitude effect. The Hautes Fagnes area has a lower g value than points situated at the same latitude but at lower altitude. The relation between g and altitude is conspicuous in valleys, e.g. the Meuse valley near Liège. The maximum variation is between Knokke and Arlon.

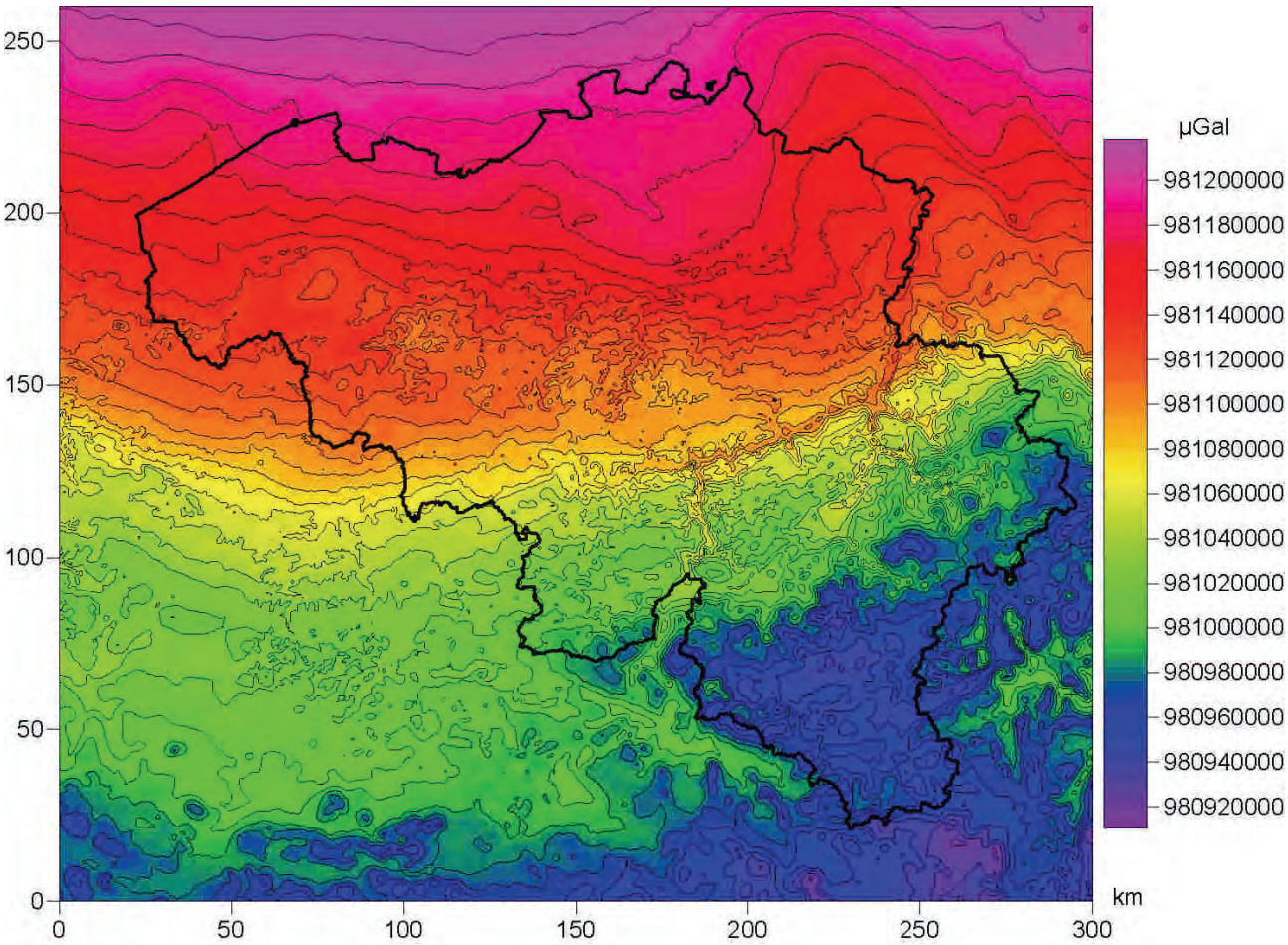

Figure 26. Map of the measured value of g, with only diurnal corrections applied (2011, this work). Explanation see text.

2.2.21. Map[m34] of the gravity measurement points

Figure 27 shows the points where gravity has been measured in Belgium. It can be appreciated that collection of the data has been done in different ways with varying density coverage. At first, measurements were made along roads, visible on the map as black paths. This method, which was used until the seventies, has the strong disadvantage to oversample along the roads and undersample off the roads. More recent networks were measured in random grids with points spread out evenly over the countryside or in built-up areas, with a density coverage depending on the available budget. The center of the country is well covered, with dense networks of 1 point/km².The Brussels region is covered with 2.5 points/km². The Ardennes and the Eeklo area have a less dense coverage of 1 point/5km². The area of Diksmuide in West-Flanders is exceptionally well covered. The offshore area is covered by a marine network of more than 38 000 points. As we can see a weak point in the raw data is the low density coverage in the Ardennes and in the western part of the Hainaut. Improving this

coverage especially in the hilly part will be of great benefit for the accuracy of the geoid and also for the geological interpretation in those zones.

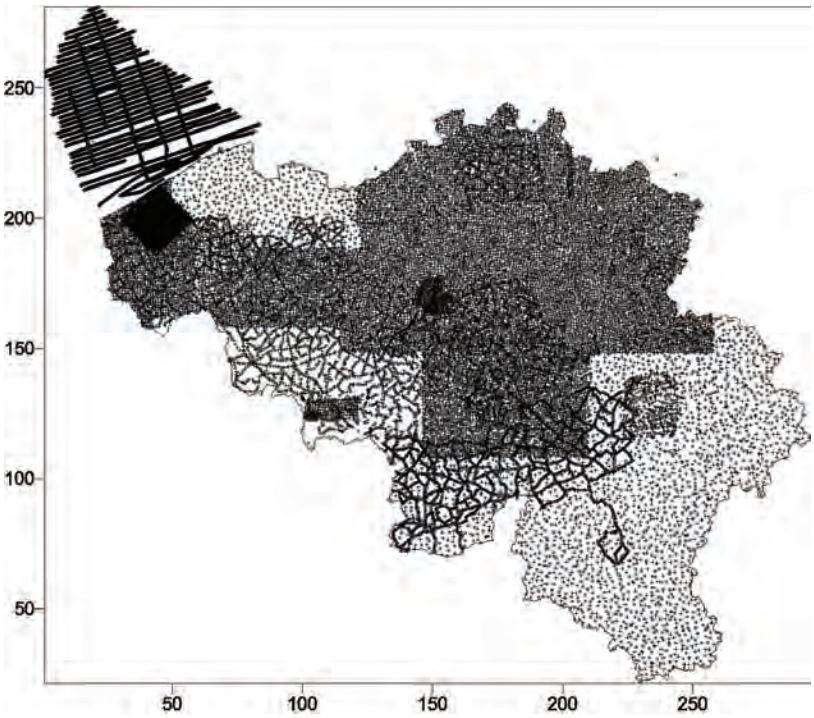

Figure 27. Map of present-day coverage of Belgium for gravity measurements (2011).

5. Calculation of a new Bouguer anomaly map with varying reduction density.

1.20. Introduction[m35]

The Bouguer anomaly map is designed to give an image of the relative density of the deeper rocks, corrected to the reference spheroid at sea level. After correcting for latitude, this still requires applying two corrections in each point (Dobrin, 1976; Telford et al., 1990). First, the free-air correction compensates for the fact that attraction of gravity above sea level decreases with height because the distance from the earth's center increases; this is proportional to the height above sea level. Second, the gravity attraction of the material between the elevation of the station (or altitude h) and sea level has to be subtracted; this is called the Bouguer correction, and the density ascribed to this material is called the reduction density. The resulting map is the Bouguer anomaly map. Until recently (see chapter 2 above), Bouguer anomaly maps for Belgium were computed using a classical reduction density of 2.67 g/cm³. Unfortunately this value is applicable only in the southern part of the country where Palaeozoic rocks are present between sea level and the level of topography. In the north, the Palaeozoic "bedrock" is overlain by soft sediments of Cenozoic age, for which a density of 2.10 g/cm³ is usually applied. When a wrong density reduction is applied for the Bouguer correction, false Bouguer anomalies are apparent due to effects of topography. For this reason, mapping the whole country with the same density correction leads to false anomalies either in the south or in the north. So until now for high-quality geological interpretation we generally used two complementary maps for Belgium, with a different density for the Bouguer correction.

In the central part of the country, the top of the bedrock dips to the north under the younger sediments from a situation near the Meuse where the Palaeozoic is present at the level of the outcrop (i.e. topography), to a more northerly situation where the bedrock dips below sea level, under soft sediments. Ideally in this intermediate zone the Bouguer correction should show a gradual transition between 2.67 in the south and 2.10 in the north, following the changing ratio of both rock types. Jones

(1951) published a Bouguer anomaly map of Belgium in which he applied a simple solution to this problem. He defined a single line from Mouscron in the west, running south of Brussels, to a point north of Visé in the east. To the north of this line he applied a density reduction of 2.1 g/cm³. Between this line and the axis of the Sambre-Meuse valleys, he applied a density which was effectively a linear interpolation between 2.1 and 2.65 g/cm³; and to the south of the axis Sambre-Meuse he used the value 2.65 g/cm³. The survey of Jones (1951) had only 381 gravity stations for all of Belgium, and only 12 stations were in the transition zone. Nowadays we have about 33000 onshore gravity stations for all of Belgium, and a few hundred in the transition zone; and the transition zone itself can be much better defined on the basis of numerous drillholes. Therefore in the present work, we use a new approach, that will be explained below.

The transition zone will be called the stacked zone, because unconsolidated cover rocks (i.e. younger sediments) are stacked on top of consolidated Palaeozoic "bedrock". It is assumed that both types of rock are present on top of each other between sea level and the local topography.

The location of geographical features mentioned in the text (cities, regions, structural features) is indicated in figure 35 at the end of the volume.

1.21. Mathematical[m36] expression of the Bouguer anomaly and the reduction density

To reach the best available solution we have to recall the definition of the Bouguer anomaly (Δg_{bg}):
$\Delta g_{bg}=g_{field}-g_0+g_{fa}-g_{bg}$
and the free-air anomaly (§ 3.4.3 Δg_{fa}):
$\Delta g_{fa}=g_{field}-g_0+g_{fa}$
g_{field} is the measured gravity g in the field, corrected for instrumental drift and earth tides,
$g_0$is the theoretical g on the reference ellipsoid (WGS84) below the observation point (this represents the latitude correction),
$g_{bg}$is the free-air correction,
$g_{fa}$is the Bouguer correction.
We notice that the Bouguer anomaly is simply the free-air anomaly minus the Bouguer correction, where
$\Delta g_{bg}=\Delta g_{fa}-g_{bg}$
There is no rock density effect on the free-air anomaly; the density only affects the Bouguer correction.
The definition of the Bouguer correction (§ 3.4.4) is
$g_{bg}=2\pi G\rho H$
where G is the gravitational constant 6.672 10^{-3} (in mGal).
In the stacked zone,
$\rho H= \rho_c(H_c)+\rho_b(H_b)$
where ρ_c is the density of the cover rocks, and $H_c$is the height of the cover; ρ_b is the density of the bedrock and $H_b$is the height of the bedrock between sea level and the cover (fig.28). ρH is the weighted density to be applied in the Bouguer correction.

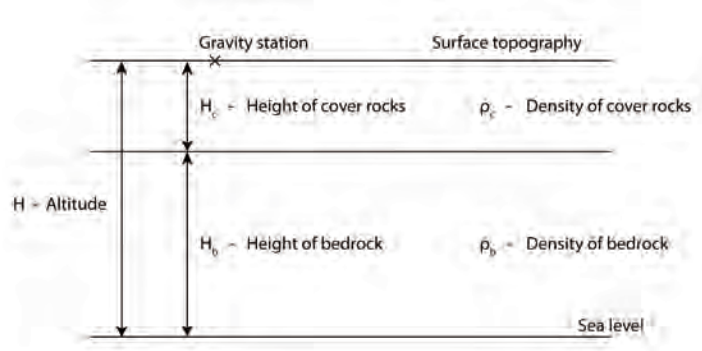

Fig 28. Schematic density profile above sea level in area with both bedrock and cover rocks (stacked zone).

Substituting g_{bg} in $\Delta g_{bg}=\Delta g_{fa}-g_{bg}$ results in:

$\Delta g_{bg}=\Delta g_{fa}-2\pi G(\rho_c(H_c)+\rho_b(H_b))$

And

$\rho=(\rho_c(H_c)+\rho_b(H_b))/H$

The weighted density ρH is the reduction density for the Bouguer correction. This reduction density will be mapped in order to visually display the results of our calculations.

1.22. Topographic[m37] map of the bedrock and of the cover rocks

As stated above, the Bouguer correction is applicable only to the mass which is present between sea level (the zero level) and the altitude H of the surface topography. As this mass can be all Palaeozoic bedrock, or all cover rock, or a stack of both rock types, we will split the area in three different areas accordingly. The stacked zone lies between the other areas. In addition to the topography of the earth's surface, we use a topographic (or bathymetric) map of the top of the Palaeozoic rocks, for all of Belgium and neighbouring areas.

First we have to define the area of the stacked zone. So, the first step in our calculation involves a file with bathymetric values of the top of the bedrock for the Brabant Massif, i.e. the Lower Palaeozoic rocks underlying most of northern Belgium, below the Cretaceous and Cenozoic cover. The area where the Brabant Massif rises above sea level is located in the south and south-east of this massif. We selected only the drillholes where the top of the Palaeozoic bedrock is at an altitude above sea level, and where at the same time soft sediment cover is present above the bedrock. These all happen to lie in a rectangle defined by Lambert coordinates 108 < X < 230 km and 145 < Y < 168 km (Belgian Lambert 72 system). South of this rectangle, the Palaeozoic is exposed at the surface. Further calculations will be focused on this rectangle, which corresponds to the stacked zone, the final objective being to estimate the weighted density ρH in each gravity observation point of this zone, as explained above. It is also observed that all drillholes within this rectangle were drilled from topographic altitudes between sea level and + 95 m.

The second step involves the gravity file of Belgium and neighbouring areas. Indeed, every gravity measurement is accompanied by a precise altitude measurement (within 2 cm), and we now construct the topographic map of these altitudes (H) by kriging (Matheron G 1962-63) with a gridding file of 1 km (fig. 28).

For our purpose, as a third step we now remove from this map all altitudes lower than +100 m, which should correspond to areas where soft sediments are present above sea level. The remainder of the map (not shown here) is the part where the Bouguer correction should be based on a density 2.67 g/cm³ in the south of the country. However, the Meuse valley, which has a topographical altitude between 0 and 100 m, was wrongly removed in this procedure, because only a negligible thickness of younger sediments overlies the bedrock; in order to correct this, a polygon is cut around the Meuse

valley using the Surfer software, and the original topographic data are restored. A similar correction is carried out in a small area in northern France, west of the Sambre-Meuse axis. Inside this temporary map, we cut out an enlarged rectangular space corresponding to the stacked zone, but slightly larger (X between 103 and 235, and Y between 140 and 173, i.e. 5 km larger than the rectangle defined above).The larger outline with a width of 5 km is effectively blanked in the grid.

Now, in a fourth step, we select from the drillhole file all drillholes where the top of the Palaeozoic is above sea level (by definition, they all lie in the rectangular stacked zone). We perform a kriging in this stacked zone, with a grid size of 1 km, which yields a smoothed map of the top of the Palaeozoic in the stacked zone. Along the border of the stacked zone, certain areas have no drillholes, so they are removed from the gridding file; in this way the blanked zone between the stacked zone and the southern part of the map is locally wider than 5 km. The fifth step involves joining the two datasets: the gridding file of the stacked zone and the gridding file of the southern part; on this joined dataset, a new kriging is carried out, which yields a smooth transition between the stacked zone and the south with its Palaeozoic outcrop. This map is the map of the topographic height of the Palaeozoic bedrock (H_b), where this is above sea level (figure 29).

The sixth step is the calculation of the topographic map of the cover rocks (figure 31), which is obtained by subtracting the topography of the bedrock (figure30) from the total topography map (figure 29). Because of our approach, this will fill in the northern part of the map and the stacked zone.

1.23. The[m38] Bouguer correction and Bouguer anomaly map

We now proceed to calculate the Bouguer correction using the formulaabove$2\pi G(\rho_c(H_c)+\rho_b(H_b))$. In the northern zone H_b is zero, in the southern zone H_c is zero, and only in the stacked zone both terms are present.The next step is the calculation of the Bouguer anomaly, by subtracting the Bouguer correction from the free air anomaly (figure 25). As explained above,

$$\Delta g_{bg} = \Delta g_{fa} - 2\pi G(\rho_c(H_c)+\rho_b(H_b))$$

This is the mathematical expression of the Bouguer anomaly map. The map is presented in figure 33.

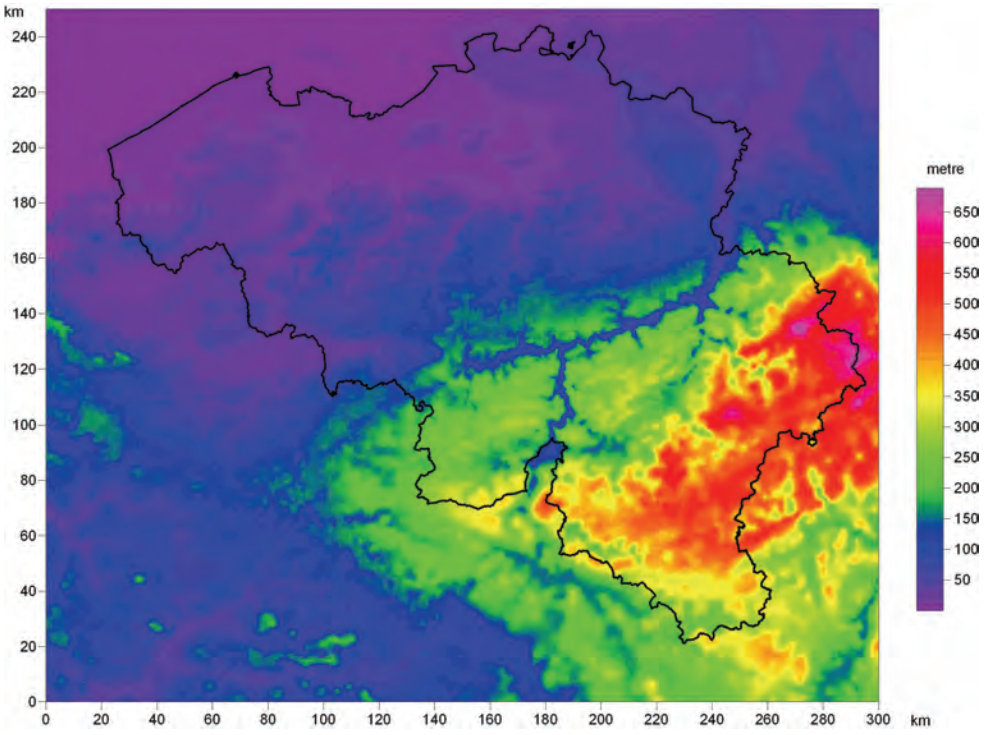

Figure 29. Topographic map of altitude H based on high-precision altimetry from gravity observation points[m39].

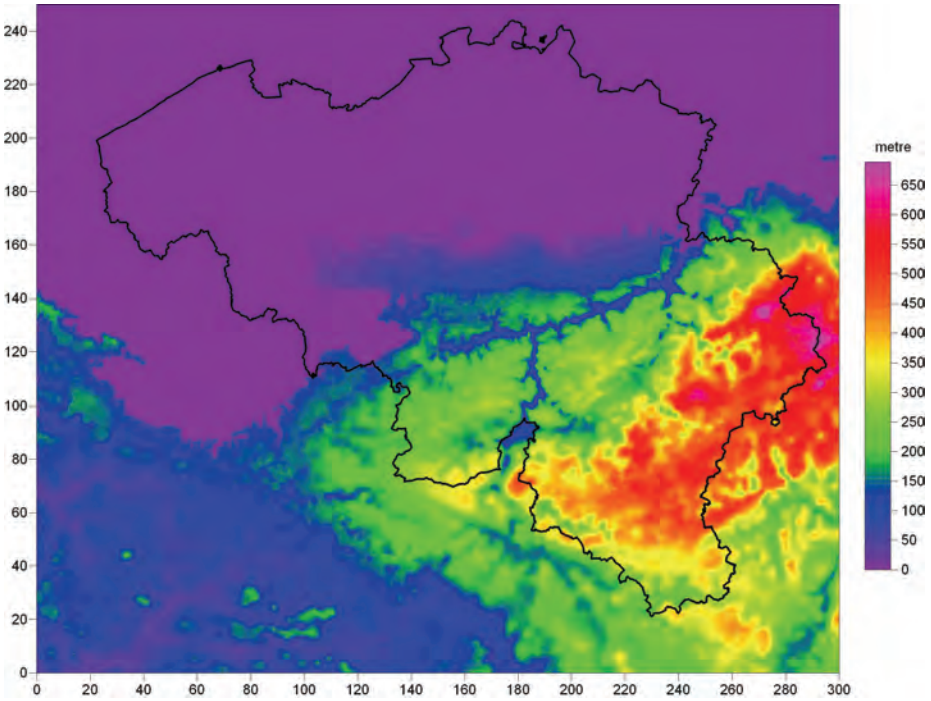

Figure 30. Topography of the top of the Palaeozoic bedrock, H_b, where this is above sea level.

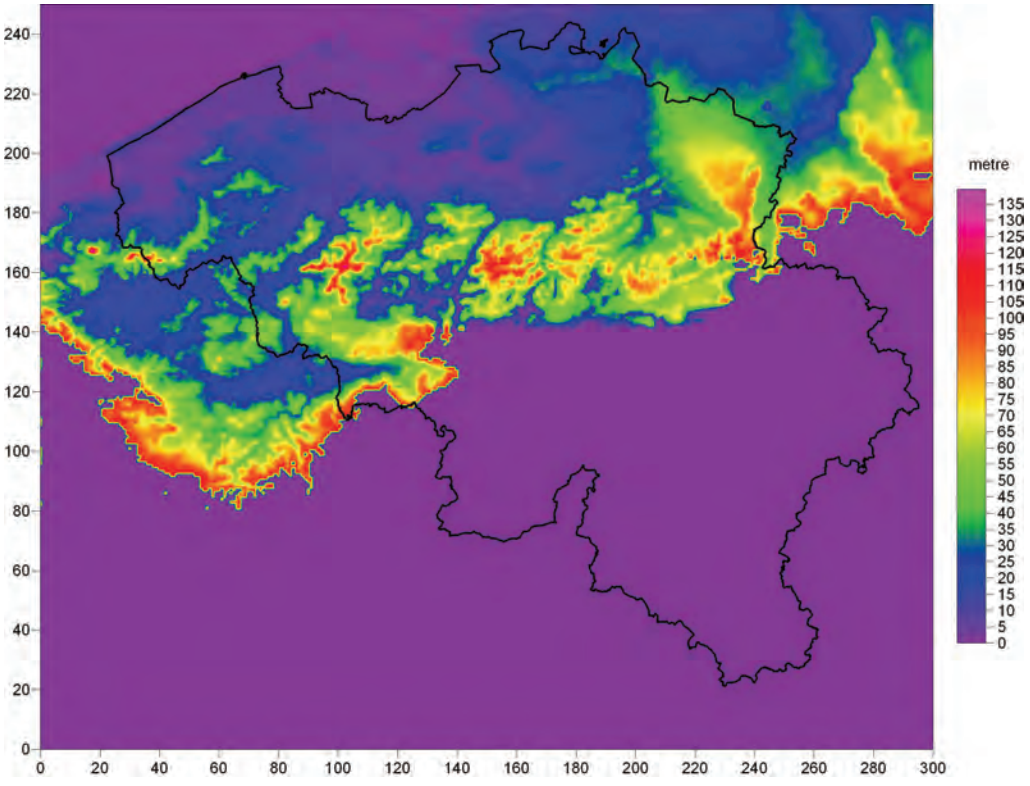

Figure 31. Cover map: topography of sediments younger than the Palaeozoic.

1.24. Density[m40] map

Finally, we can make a map of the weighted density values used for the reduction density of the Bouguer correction, as explained above, $\rho=(\rho_c(H_c)+\rho_b(H_b))/H$.

As we can see on the density map (figure 32), a reduction density of 2.1 g/cm³ is applied in the northern part of the country, in northern France and in the Netherlands. The first Bouguer anomaly map calculated for the Netherlands was already calculated with a density of 2.1 g/cm³ (Jones, 1951). For the Ardennes area the classical value of 2.67 g/cm³was used. The most interesting feature on this map is the stacked zone, where a gradual increase of the reduction density can be appreciated from 2.1 g/cm³ in the north to 2.67 g/cm³ in the south, as the Palaeozoic fills a larger proportion of the space between sea level and the topographic altitude.

Figure 33 shows an overlay of the Bouguer anomaly contour map on top of the colour-coded density map.

Figure 34 presents the new Bouguer anomaly map calculated with the varying reduction density. This map will be discussed in more detail in the next chapter.

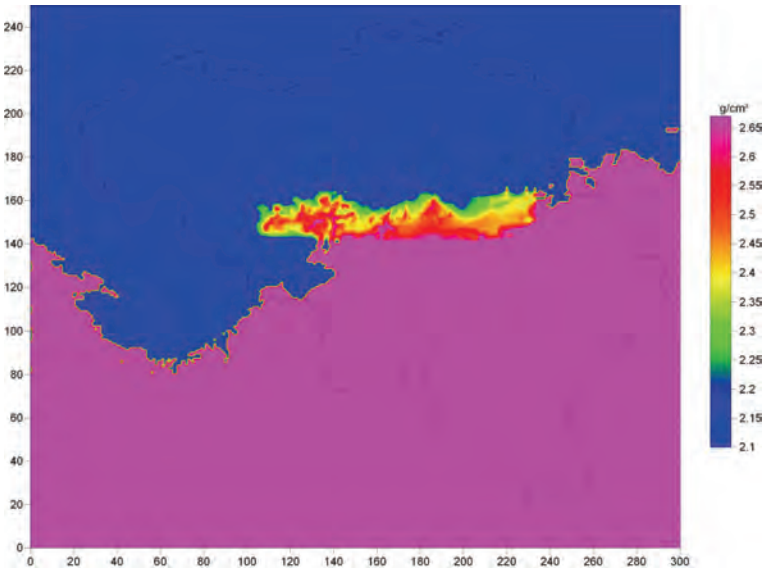

Figure 32. Reduction density map used for the Bouguer correction, i.e. for rocks between sea level and topography.

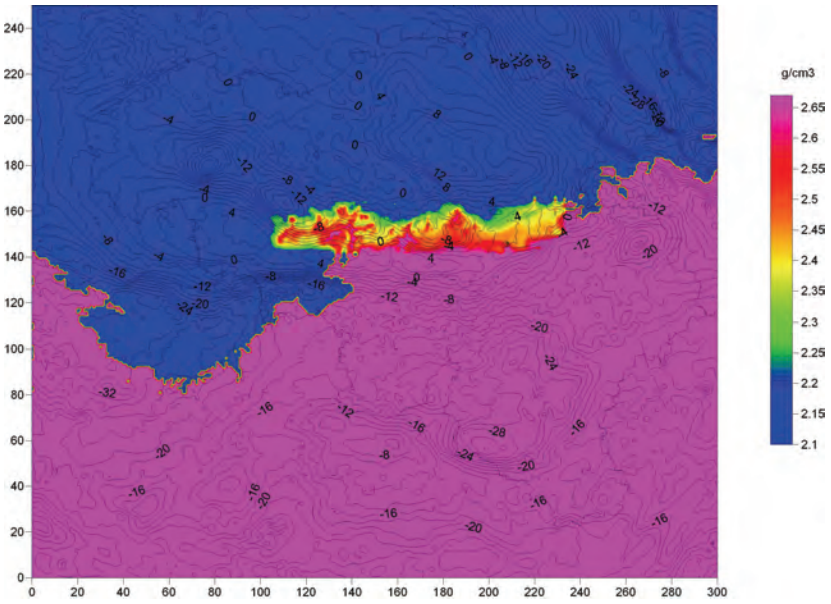

Figure 33. Overlay of the Bouguer anomaly contour map on top of the colour-coded density map.

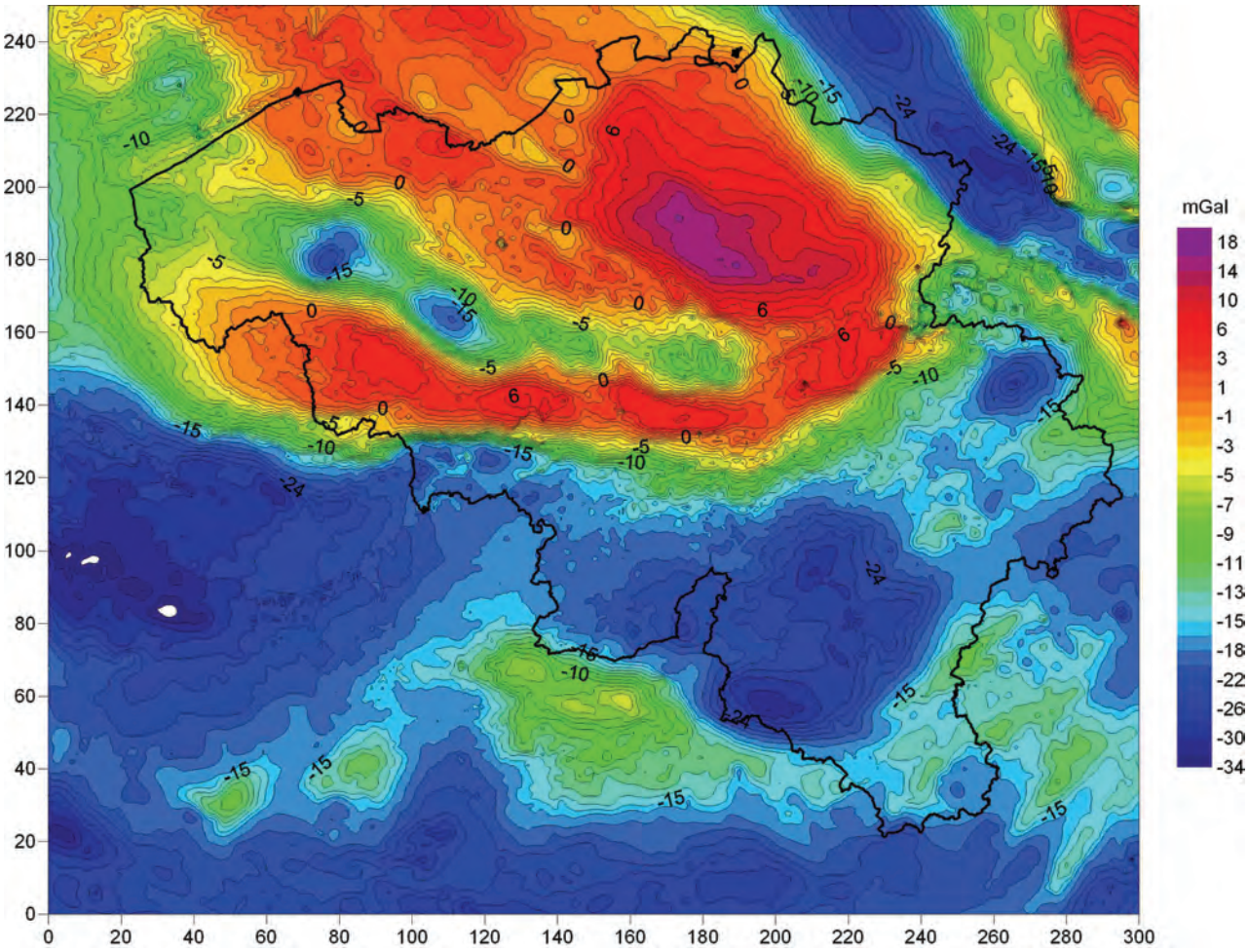

Figure 34. Bouguer anomaly map of Belgium calculated with varying reduction density (2011, this work[m41]*).*

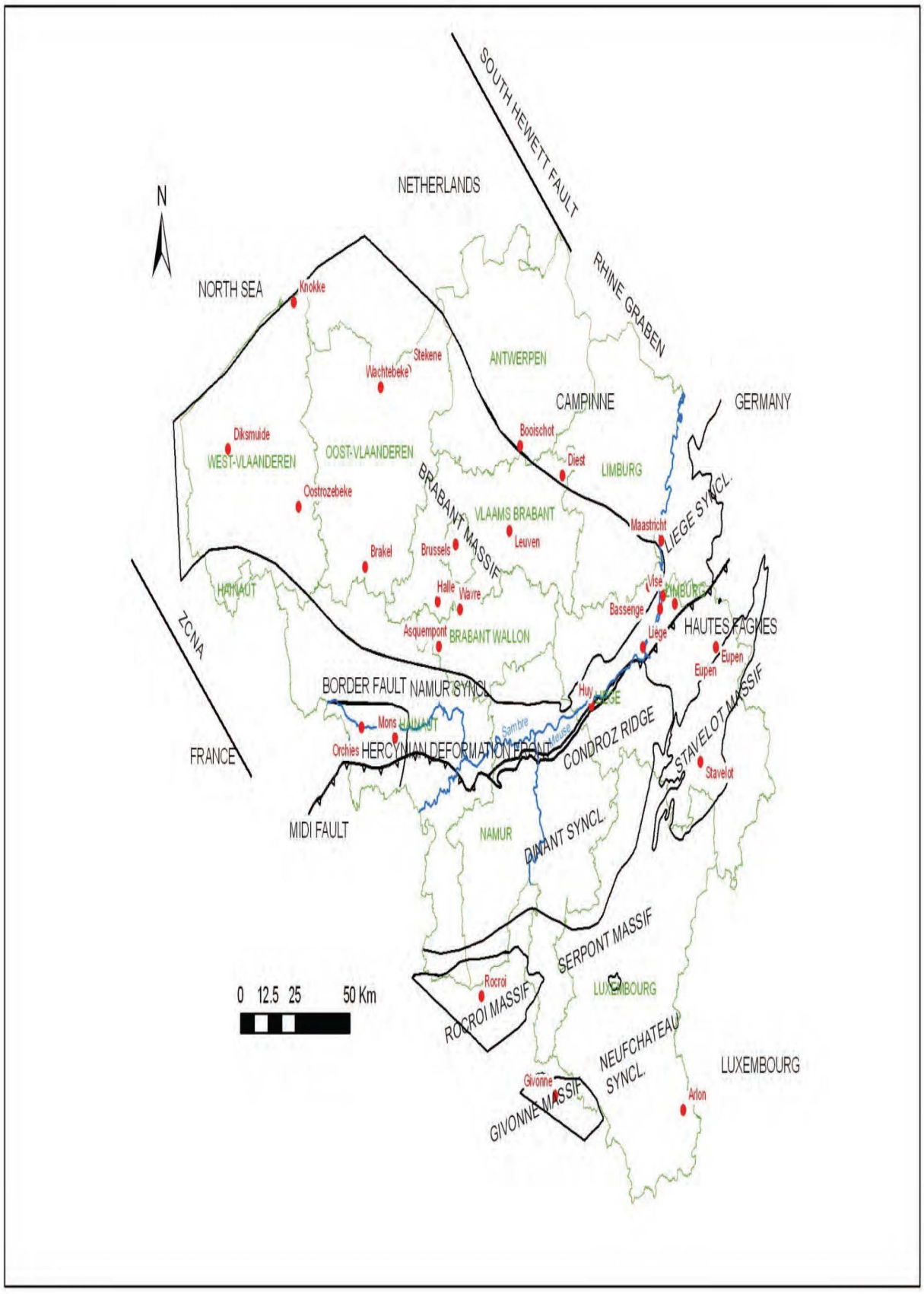

Figure 35. Location of geographical features mentioned in the text (cities, regions, structural features[m42]*).*

6. Interpretation of the Bouguer anomaly map of Belgium

1.25. Review[m43] of literature concerning gravity in Belgium.

Note: the location of geographical features mentioned in this chapter (cities, regions, structural features) is indicated in figure 35.

The first publication addressing the geological structure underlying gravity anomalies in Belgium was by Souriau (1979). She studied the upper mantle below the Paris Basin and the Benelux, based on the analysis of P-wave residuals caused by nuclear explosions, and on Rayleigh waves. She draws a parallel with structures observed in rift systems, specifying that these cannot be explained by variations in the crust, but that the mantle has to be involved. Two particular structures are outlined : one from the south-east of Belgium to Luxembourg and the other one to the north-east of Brussels. According to her hypothesis, partially melted mantle, heavier than crustal rock, was upwelled beneath a zone from Luxembourg to the Eifel, where it was manifested in volcanism.
The positive anomaly found to the north-east of Brussels on the gravity map of Jones (1948) could be the result of a mantle upwelling of up to 20 km, with thinning of the crust, which could explain the anomaly in seismic P-wave velocity (Souriau, 1979).

The negative anomaly of Flanders was first discussed by De Meyer (1983, 1984). The density contrast and the shape of the bodies were determined purely numerically. Either a granitic intrusion or a sedimentary basin can satisfactorily explain the anomalies. The model is not constrained by the real geology[m44].

Bouckaert et al. (1988) discuss the results of the deep seismic profile BELCORP and mention two anomalies in the gravity map along the seismic line: a negative one in the south, which they explain based on De Meyer's idea (1984), and a positive one for which they invoke Souriau's interpretation (1979). They also mention mantle upwelling and link this to a possible hot spot associated with the Eifel volcanism.

The density and magnetic susceptibility of 62 samples from different lithologies in the Brabant Massif were determined by De Vos et al. (1992), as a contribution to gravity and magnetic modelling. This is of particular importance for understanding the Flanders anomaly. In a joint effort, the Geological Survey of Belgium and the British Geological Survey modelled two profiles through Belgium in 2.5 D, attributing density and magnetic susceptibility values to polygons representing rock formations in the underground (Chacksfield et al., 1993). This is the first modelling based on geologically realistic rocks that fill the crustal space. Gravity data were taken from Jones (1948), magnetic data from the aeromagnetic survey conducted by the Geological Survey of Belgium (BGD/SGB, 1964), and digitised for this occasion. The first profile crosses the Brabant Massif from south-west to north-east through the negative gravity anomaly of Flanders, which is interpreted as an intrusion of an acidic body. The second profile crosses the south-east of the country, where a negative gravity anomaly coinciding with a positive magnetic anomaly is attributed to a deep-seated light magnetic body under the Ardennes. The large wavelength of the anomaly points to a deep-seated body, which is inferred to be Precambrian, in analogy to the south of England. The maps of magnetism and gravity are published as a separate booklet (De Vos et al., 1993); for the gravity map based on Jones (1948) the data were here reduced with a density of 2.74 g/cm³ , a figure that is too high for Belgium, which may result in false anomalies.

Pharaoh et. al. (1993),in their introduction to the special issue of Geological Magazine on the Caledonides of the Anglo-Brabant Massif, state that using data which can 'penetrate' the thin cover of Upper Palaeozoic, Mesozoic and Tertiary strata, geophysical studies make a fundamental contribution to the knowledge and structure of this massif, by enabling the construction of crustal models based on integration of potential field, seismic and geological data.

The Belgian gravity data were integrated with the British data by Lee et al. (1993), showing structures

of the Anglo-Brabant Massif at a larger scale. Geophysical lineaments oriented SSE define limits of blocks in the upper crust. An off-shore N-S seismic profile located to the north-east of the Anglo-Brabant Massif (the BIRPS-MOBIL-7) was interpreted using seismic, gravity and magnetic data. It is deduced that the upper crust is non-reflective and mainly non-magnetic, interpreted to be a Caledonian fold-thrust belt. The middle crust has varying magnetic susceptibility and reflectivity, and is interpreted to be an imbricated thrust stack with properties similar to the Tubize group from the Lower Cambrian in Belgium. This mid-crustal magnetic body, situated at the north-eastern edge of the Brabant Massif, lies on top of a seismic reflector plunging to the southwest into the lower crust, and brought in relation with the South Hewett Fault in Britain.

Hennebert (1993) mentions the effect of isostatic buoyancy, resulting from the presence of lighter rocks in the heart of the Brabant Massif, on later deformation and younger basin formation. He deduces that the low-density body of Flanders is rigid and follows De Meyer (1984) in proposing ahypothetical granite. The obliqueness of the granitic axis with respect to the Zone de Cisaillement Nord-Artois (ZNCA) and to the Border Fault (Faille Bordière of Legrand, 1968) created rapidly subsiding transtensional basins between the two structures, e.g. the “Auge Hennuyère” with thick Devonian-Carboniferous sediments to the south of the gravity anomaly. This process continued into the Meso-Cenozoic in the Mons Basin.

Verniers & De Vos (1995) give an overview of recent research in the Brabant Massif in Belgium in the fields of stratigraphy, palaeogeography, and the acquisition of gravity and magnetic data. For magnetism attention is drawn to the Tubize group rocks as being responsible for most of the positive magnetic anomaly. For gravity the authors explain the positive anomaly of the overall Anglo-Brabant Massif as a thick wedge of fine-grained sediments of Ordovician-Silurian age, extending from Belgium to East Anglia.

Everaerts et al. (1996) carried out a mathematical modelling over the gravity low of Flanders, integrating recent geological mapping (De Vos et al., 1993), petrophysical data (De Vos et al., 1992) and geophysical data, among them a dense network of recently acquired gravity points. They used the GravMag software developed by the British Geological Survey (Pedley, 1991).The negative anomaly is best explained by a granitic batholith. This body has a width of 15 to 20 km and a length of about 70 km. The shallower parts have a roof at a depth of about 1.5 to 2 km and are located in Oostrozebeke and Brakel. Near Oudenaarde the depth of the roof is inferred to be 5 km. A crustal intrusion up to 15 km depth is compatible with the model. The 2.63 g/cm³ used for the model is similar to the density of inferred granites in eastern England and in the Lake District (Lee, 1989). Using the second vertical derivative of the gravity field, a model was proposed for the shape and depth of the intrusion. This procedure shows lineaments which have an edge that is almost vertical in the west and oriented WNW-ESE and SW-NE in the south. These are probably vertical faults. In the north however the edge of the granitic intrusion is sloping. The granite is broken by transverse faults. The shape of the intrusion and the relation with the surrounding rocks seem to point to an active contribution to later deformation, according to the authors.

Van Grootel et. al. (1997) present a review of the basin development, subduction-related magmatism, deformation and metamorphism of the Anglo-Brabant fold belt in the context of Eastern Avalonia. The proposed model would imply the existence of two subduction zones related to the Avalonia-Baltica collision, one of them lying along the Anglo-Brabant fold belt. This publication describes both interstratified and intruded volcanic rocks in the Brabant Massif , but does not mention a possible link with a granitic intrusion. The basin inversion and collision in the Middle Devonian created the general antiform structure of the Anglo-Brabant fold belt, which is expressed as a positive gravity anomaly due to stacking of thrust units containing fine-grained high-density sediments.

De Vos (1997a) associates the granitic intrusion with the crustal subduction under Avalonia at the end of the Ordovician or the beginning of the Silurian (445-425 My). The author also notes that the intrusion probably blocked the Acadian deformation dated at about 400 My. As this presentation was made in the framework of a symposium on economic and ecologic applications of the deep

underground of Flanders, the author mentions three possible societal applications for the granitic intrusion: production of geothermal energy, mineralisations, and storage of nuclear waste. It is also mentioned that gravity measurements are used to calculate the geoid. The gravity contrast between rocks of Ordovician-Silurian age in northern Belgium and Devonian-Carboniferous rocks in southern Belgium is also highlighted, with an explicitly traced gravity gradient south of the Sambre-Meuse axis. Also explicitly mentioned are different negative gravity anomalies aligned from Diksmuide over Oostrozebeke, Brakel and Halle to Wavre, all hypothetical granitic batholiths. Transverse faults through the granitic bodies, oriented SW-NE, are seismogenic zones in the present Quaternary period.

De Vos (1997b) is a similar review of everything that is known about the gravity anomalies of Flanders and their possible explanation by granite intrusions. The influence on Acadian and later deformation is discussed. In particular, Kimmerian deformation (Trias-Jurassic) generated transverse faulting with vertical and horizontal displacements; lighter blocks became horsts. The longitudinal axis of the granite corresponds to a horst on the bedrock map, while a smaller block centered on Oostrozebeke seems to form a transverse horst.

De Vos (1998) gives a short history of the Brabant Massif, summing up previous literature data, including gravity data, for which no new hypotheses are presented.

Everaerts and Hennebert (1998) analyse the gravity data for the French-Belgian border zone along the Variscan front. Different mathematical filters were applied to the data to better understand the structural setting of the area. The first vertical derivative and the horizontal derivative were computed. The analysis shows that the Mélantois-Tournaisis and the Orchie Palaeozoic Anticlines belong to the same structure. This flower structure has shaped the Midi Fault in its southern part. This structure could be a link between the Nord-Artois Faulted Zone and the Border Fault north of the Mons Basin. The “Border Fault” is not matched by a lithological contrast at depth. The first vertical derivative map is very enlightening, as it underlines the extension of the coal basin, characterised by low density rocks that are well marked on the gravity map.

Oulidi (1998) used the GravMag software from the BGS to model a few profiles across the Brabant Massif and its southern edge. He confirms the occurrence of the granitic intrusion and models it in three dimensions. He explains the strong positive anomaly in Flanders (Bouckaert, 1988) by an upwelling of the mantle.

Sintubin (1997b) proposes a tectonic escape model based on an analysis of magnetic lineaments, to explain the different directions of these lineaments. Among other conclusions, the following is related to the gravity anomaly: the southern part of the Cambrian core of the Brabant Massif shows a central magnetic ridge which can be interpreted as a major dextral transpressive shear zone; movement of this Cambrian core to the southwest is obstructed by a granitic batholith, whereby the author refers to Chackfield et al. (1993), Everaerts et al. (1996) and De Vos (1997).

Using aeromagnetic data and field geological data, Sintubin (1997a, 1999) notes different types of cleavage-fold relationship. The curvature of both cleavage and fold trajectories reflect the specific architecture of the Cambrian core acting as an indenter during the Acadian deformation of the Ordovician-Silurian basin which is wrapped around the Cambrian core. This shows a link with the granitic intrusion deduced from the gravity pattern. The author shows that small Bouguer anomalies, which are satellites of the main Flanders anomaly, seem to be displaced dextrally with regard to the main anomaly. The author works out the indenter model, with the granite being a buffer against which the deformation abuts. He does not exclude a Cadomian age for the basement, following geochemical studies by André (1991).

Mansy et al.(1997)present an interpretation of a seismic profile south of Valenciennes along a meridian situated at 3°36’30”, crossing the Variscan deformation front. Different seismic reflectors are found, and the model is validated by gravity measurements and knowledge of the rock densities. The main conclusion is that the steep gravity gradient between the south and the north is due to the sudden

deepening of the Brabant Massif, but a new idea worked out in this profile, in accordance with gravity data, is to put high-density material (as in the case of Lower Palaeozoic rocks) on top of lower-density material (Upper Palaeozoic rocks), both being separated by the Midi thrust fault. This reflects the structural position of the Condroz inlier more to the east.

Mansy et al.(1999) publish a detailed gravity map showing the existing dense coverage in some areas, as well as the magnetic anomaly map based on the 1993 aeromagnetic measurements, as a geophysical background to a geological-structural framework of Belgium. On the gravity map we see the contrast between the Lower Palaeozoicin the northern subdomain, and the Upper Palaeozoic in the southern subdomain. The southern subdomain, without magnetic rocks, is moulded around the granitic core, whereas a northern subdomain, containing the Cambrian magnetic metasediments, shows numerous thrust faults towards the south over the granites.
The Brabant Massif also acted as a barrier during the Variscan deformation in the south of the country. Mansy et al. (1999) attribute the positive gravity anomaly of the Brabant Massif to the high-density pelitic sediments of the Ordovician-Silurian sedimentation cycle folded during the Acadian. They note that the large negative gravity anomaly in the south of the Brabant Massif, modelled as a granitic batholith, is elongated WNW, and that this direction corresponds to the orientation of the massif itself. To the south and south-east of the gravity high of the Brabant Massif, the Artois and the Ardennes regions appear as gravity lows, with an even lower anomaly underlying the Rocroi Massif and the Boulonnais.
A characteristic of the map is the horizontal gravity gradient between the Ardennes in the south and the Brabant Massif in the north. North of the Mons Basin this gradient is very steep. In the Namur region the gradient passes from an E-W direction to a SW-NE direction, up to Visé, and more to the east the gradient is cut off by the Rhine graben. Towards the west, the gradient takes a NW direction to the west of Saint-Amand, the gradient gradually loses its abrupt character and reaches the coast between Nieuwpoort and Dunkerque. Despite the seismic similarity of the southern and northern subdomains (characterised by an absence of reflectors), and despite the fact that the vertical extension of the faults associated with this boundary is unknown, the gradient represents a crustal boundary. The authors explain that the gravity gradient represents the most reliable boundary of the Brabant Massif at depth.
From the gravity map, the authors deduce that the south edge of the Brabant Massif is very steep, and reflects the large density contrast between the Ordovician-Silurian metasediments in the north and the low-density Devono-Carboniferous sediments in the south. Towards the west, the Brabant Massif is more gently dipping below younger sediments. The south-east and the north-east borders have an intermediate behaviour.
The authors interpret the curved trend of the negative gravity anomaly as an arc-shaped succession of granitic batholiths. Thus, the anomaly with two minima at Halle and Wavre is defined as the Halle-Wavre granite. Similarly the anomaly of Maastricht is considered to be a granite since it is in the eastern prolongation of the gravity anomalies of the Brabant Massif. And towards the west, the negative Bouguer anomaly on the Belgian continental shelf is also interpreted as a granite; it had been interpreted as a magmatic body in a seismic profile (Rijkers et al., 1993). The depth of the roof is estimated at 2 km depth in Oostrozebeke and Brakel, following the modelling by Everaerts et al. (1996) and at about 5 km, based on the intensity of the anomaly, at Halle-Wavre, Maastricht and on the continental shelf. They note that the Halle batholith seems to be displaced to the NW with respect to the Brakel granite along a NW-SE strike-slip fault; in turn the Wavre granite is displaced with respect to the Halle granite along a fault with the same trend. Again it is stated that the granitic batholiths constituted a rigid crustal basement affecting later folding events.

Everaerts (2000) applies a filter in the Fourier domain on gravity and magnetic maps, and draws some structural conclusions on the Brabant Massif. He confirms the occurrence of strike-slip faults in the tectonic model, the close relationship between magnetic and gravity features in the centre of the massif, and the subvertical position of the Cambrian strata.
Pursuing this theme further, Sintubin & Everaerts (2002) propose a compressional wedge model for the Anglo-Brabant deformation belt based on potential field data. Field observations only allow kinematic inferences to be made for the southern part of the Brabant Massif, the remaining part being

hidden under younger cover. On the other hand, potential field data (aeromagnetism and gravity) enable to complete the picture. They not only corroborate the kinematics, but also reveal the key players in the late Silurian to early Devonian that caused the observed architecture of the orogeny. Crystalline basement blocks, most probably of Precambrian age, controlled the kinematics. Finally it is suggested that the development of a rift or pull apart basin in a transtensional inter-continental setting during the Cambrian may have been crucial in the subsequent deformation history of the Anglo-Brabant belt.

Verniers et al. (2002) present a synthesis on the development and evolution of the Anglo-Brabant Deformation Belt (its new formal name), where Belgian gravity data were set in a larger context, integrating parts of France, England and Germany. On this extended gravity map,the Bray fault in the north of the Paris Basin clearly marks the southern edge of the micro-continent Avalonia.

Debacker et al. (2004) describe two fold types in the Brabant Massif, the transition between them, and their genesis. The fold type in any particular area depends on its spatial position with respectto the Asquempont lineament, just to the north-east of the gravity low of Brakel. The authors stress the importance of the low-density body at depth in influencing the deformation process.

Wiliamson et al. (2004) describe the interpretation of gravity anomaly data over the Brabant Massif in southern Flanders. The gravity lineaments show a predominant WNW-ESE trend, with a notable absence of significant features with a SW-NE trend.2.5D modelling confirms the hypothesis of a granitic intrusion. A 3D modelling was carried out, using a space-domain, prism-based method to adjust automatically the top and/or base of a modelled unit, and this technique is iterated until an optimal result is reached. In this way, a depth was obtained for the roof and the base of the low-density body. The depth of the roof varies from 2000m for the western anomaly to 4000 min the east. The base was modelled at 11000 to 7000 m. This means a (vertical) thickness of about 9000 m where the anomaly is largest, and 3000 m where the anomaly is weaker. Euler deconvolution was also calculated to estimate the depth of the low-density body. This method requires a structural index; with a structural index of 1 (corresponding to a “cylindrical” body lying horizontally, which is the most plausible geometrical situation for an elongated intrusion) the authors obtain depth values which are very similar to the 2.5D and 3Dmodelling. This reportalso concludes that the intrusive body underwent a dextral displacement.

1.26. Interpretation[m45] of the new Bouguer anomaly map 2011

The present high-density gravity coverage of the country has been completed in 2002. A synthesis for the whole country was already presented by Mansy et al. (1999), as discussed above, at a time when some areas were still insufficiently covered, notably in the north-east and the south-east where only the data from Jones (1948) were available. Nevertheless the gravity interpretation published by Mansy et al. (1999) is still generally valid.

The main features of the Bouguer anomaly map of Belgium have been known for some time: the positive anomaly in the northern part of the country corresponding to the Brabant Massif, the negative anomaly in the Ardenne area, the rather sharp gradient between these two different structural units, the negative anomaly corresponding to the Rhine graben in the north-east, and the arc-shaped succession of gravity lows in the southern part of the Brabant Massif. The latest gravity acquisitions and the present novel calculation of the Bouguer correction with a variable density (see above, chapter 5), enable us to see some features in more detail, and the text below will focus on these areas.

A feature which is well documented in the present map (figure 34) is the strong positive gravity anomaly to the north of Leuven, elongated in a WNW-ESE direction, about 20 km wide and 50 km long, delimited by a strong gradient in the south-west, and decreasing more gradually towards the north-east. One possible explanation is the presence of thick fine-grained metasediments of Ordovician-Silurian age, which have been put in subvertical position by the Acadian (Brabantian)

deformation. Towards the south-west only coarse-grained metasediments of Cambrian age are present (Piessens et al., 2005), with a lower-than-average density, which explains the gravity gradient. Moreover, the steep border fault of the Campine roughly follows the long axis of the gravity anomaly, pointing to a continuation of the high-density rocks to the north of this fault. Undoubtedly the Ordovician-Silurian rocks continue below the fault, so they are present at greater depth towards the north-east, attenuating the gravity signal. But above the fault, a thick conglomerate was found in the Booischot drillhole, of probable Mid-Devonian age, with pebbles derived from the Silurian fine-grained metasediments, and showing a high bulk density, similar to the Silurian (De Vos et al., 1992). So this whole area potentially has a higher-than-average density, and influences the gravity signal. However, this is not the only possible explanation. As pointed out by Souriau (1979), and using seismic arguments (see above), a high-density mantle influence is not excluded, i.e. the mantle would locally be present at a higher level. This is plausible because continental fractures such as the Roermond Graben cause an upwelling of the graben rim. Probably the deeper mantle cause and the shallower fine-grained Palaeozoic metasediments add up to cause this anomaly.

In the northern part of the province of East-Flanders, and into the Netherlands, parallel elongated features are visible on the gravity map, oriented WNW-ESE. The positive anomaly seems to correspond toa syncline of Ordovician-Silurian rocks, whereas the negative anomaly corresponds to an anticline of Cambrian coarser-grained metasediments in the subcrop (Piessens et al., 2005). It should be noted that the magnetic pattern is exactly the reverse, with a stronger anomaly where the Cambrian Tubize Formation is closer to the surface. Exploration drillholes performed in 1998 and 1999 confirmed the structure that was expected on the basis of the magnetic pattern (De Vos & Verniers, 2000). At Stekene, a drillhole located in a magnetic high, i.e. a gravity low, showed turbidites of the Chevlipont Formation (Tremadocian), immediately underlain by Cambrian metasediments, whereas in a drillhole at Wachtebeke in a magnetic low, i.e. a gravity high, grey shale and hemipelagite of the Wenlock (Silurian) is present (Piessens et al., 2005).

The arc-shaped succession of gravity lows from the North Sea to Maastricht is here still interpreted as granitic intrusions, with anEarly Silurian age being the most probable, but without excluding the possibility of a Precambrian age. The gravity lows are interrupted between the Wavre granite and the Maastricht granite. East of the Wavre granite and northwest of Waremme, there is a linear structure oriented north-east to south-west, with a lower gravity signal. It follows the general trend of the Brabant Massif structure which in this area is shaped as an anticline, and the lower gravity probably corresponds to Cambrian rocks, as elsewhere in the Brabant Massif. In the area of Visé-Bassenge, close to the Dutch border, the Maastricht gravity low shows an appendix pointing into Belgium. The most likely explanation is the intrusion of granitoid rocks at depth. Volcanic rocks have been found in two drillholes near Visé (Hermalle-sous-Argenteau and Visé) and although they are not exactly on top of the gravity low, they could be genetically related to the deeper intrusion, a structural setting similar to the western Brabant Massif, where small intrusions and interstratified volcanic rocks are found in the subcrop, i.e. shallower than the intrusion causing the gravity lows, but not exactly on top of them.

As was pointed out by Chacksfield et al. (1993) the general negative gravity signature of the Ardennes coincides with a magnetic high, at the scale of the whole Ardennes massif. This is a crustal characteristic at great depth, pointing to the very nature of the Avalonian crust in the Rheno-Hercynian zone. On the new map, a very large gravity low is present under the central part of the Ardennes, with values that are about 10 mGal lower than the Ardennes average. Given its shape and amplitude, this gravity low must also correspond to a deep crustal feature.

The main trends in the gravity anomalies of the Ardennes region coincide with the Variscan deformation trends, to the west of Dinant they are oriented E-W, and to the east of Dinant SW-NE. The Lower Devonian axis generally shows a positive gravity signal. Also the synclinorium of Neufchâteau-Eifel (called Wiltz in Luxembourg) is characterised by a slightly more positive anomaly; on both sides the fold axis plunges, to the south-west and to the north-east (Ghysel, pers. comm.),

which is accompanied on the map by a decrease in gravity values. Other subtle similar features could be due to plunging fold axes.

It is to be noted that the Cambrian inliers of Rocroi and Stavelot leave no gravity signature. The Givonne anticline shows a negative anomaly superposed on the large gravity low of the central Ardennes.

A strong negative anomaly is present in the Eupen area. There is no easy explanation, but it is worth noting that the Helle tonalite crops out to the north-east of the gravity anomaly. Again, like in the Visé area and in the western Brabant Massif, the presence of magmatic rocks in outcrop could be an indication of a deeper intrusion of light granitoid rocks.

In southern Gaume where lighter Mesozoic rocks lie above denser Palaeozoic rocks, the gravity signal is rather positive, which means that the unknown deeper geology has a stronger signature than the geological features closer to the outcrop.

At the regional European scale, the Belgian gravity highs and lows are not very prominent. Nevertheless, the Anglo-Brabant gravity high accompanying the Anglo-Brabant Deformation Belt is sufficiently pronounced to leave a crustal mark, due to its thick fine-grained detrital metasediments, as it is surrounded by younger, less dense rocks (Pharaoh et al., 2006).

1.27. Conclusions[m46]

Until recently the Bouguer map of Belgium was calculated using the classical density of 2.67 g/cm³. Unfortunately this value is only valid for the south of the country where Palaeozoic rocks are present between sea level and topographic level. In the north Palaeozoic rocks are overlain by soft sediments of Meso-Cenozoic age with a mean density of 2.1 g/cm³. In the central part an area occurs where younger rocks are stacked on top of the Palaeozoic with an interface lying between sea level and the topographic height. In this area the Bouguer correction should show a gradual transition between 2.1 g/cm³ and 2.67 g/cm³. This was worked out for this publication in chapter 5, and the resulting Bouguer anomaly map with a varying reduction density was produced. This map also benefits from the high-density coverage of gravimetric measurements achieved in 2002 for Belgium. The new map shows some gravity features in more detail. Typical examples are the gravity high in the Diest area north of Leuven, and the parallel gravity lows and highs in northwest Belgium which can be explained by synclines resp. anticlines in the Lower Palaeozoic.

The major features of the gravity map have been known for a long time. They include a positive Bouguer anomaly in the north and a negative anomaly in the south of the country, with a sharp gradient in between; this represents the contrast between Lower Palaeozoic rocks in the north and Upper Palaeozoic rocks in the south. Below the Ardennes a deep crustal feature contributes to the gravity low and the magnetic high. In the north-east of Belgium the Roermond Graben (extension and part of the larger Rhine Graben) appears as a negative anomaly oriented NW-SE.

A strong positive gravity anomaly north of Leuven is interpreted as a thick accumulation, both sedimentary and structural, of fine-grained metasediments of the Ordovician-Silurian, in combination with a possible mantle upwelling to the SW of the Roermond Graben.

Parallel elongated features in the north of the province of East-Flanders and into the Netherlands can be explained by synclines of Ordovician–Silurian rocks (positive gravity anomalies) and anticlines of coarse-grained Cambrian metasediments where the Ordovician-Silurian was eroded (negative anomalies).

The arc-shaped succession of gravity lows, from Flanders over Brabant and up to Maastricht, is interpreted as a series of granitoid intrusions with a probable Silurian age. The gravity lows are interrupted between the Wavre granite and the Maastricht granite.

The main trends of the gravity anomalies in the Ardennes coincide with the Variscan deformation trends. The Lower Devonian anticlinal axis generally shows a positive gravity signal, and also the synclinorium of Neufchâteau-Eifel is characterised by a positive anomaly. In the central part of the Ardennes, a region with a gravity value about 10 mGal lower than the surroundings is attributed to a deep crustal feature. A strong negative anomaly in the Eupen area is interpreted as a granitoid intrusion at depth.

7. References

ANDRE, L. 1991. The concealed crystalline basement in Belgium and the "Brabantia" microplate concept: constraints from the Caledonian magmatic and sedimentary rocks. *Annales de la Société Géologique de Belgique* **114** (1): 117-139.

BARZAGHI, R., BORGHI, A., DUCARME, B. & EVERAERTS, M. 2003.Quasi-geoïde BG03 computation in Belgium. *Newton's Bulletin* n °1: 75-88.

BELGISCHE GEOLOGISCHE DIENST (BGD)/SERVICE GEOLOGIQUE DE BELGIQUE (SGB), 1964. Aeromagnetische kaart/Carte aéromagnétique, scale 1:300.000, printed at the Military Geografical Institute, Brussels.

BGI web (http://bgi.omp.obs-mip.fr) Bureau gravimétrique international. Formules de Réduction des données gravimétriques. Centre des données, Division de la gravité, de la géothermie et de la géodynamique, Direction de la Physique du Globe 1984.

BOUCKAERT, J., FOCK, W. & VANDENBERGHE, N. 1988. First results of the Belgian geotraverse 1986 (BELCORP). *Annales de la Société Géologique de Belgique* **111**: 279-290.

CANNIZZO, L., CERUTTI, G. & MARSON I., 1978.Absolute Gravity Measurements in Europe. *Il Nuovo Cimento*Vol 1c(1) No 1.

CARTWRIGHT, D. E.& EDDEN, A. C., 1973.Corrected tables of tidal harmonics. *The Geophysical Journal*., Vol. 3, No. 33.

CHACKSFIELD, B., DE VOS, W., D'HOOGE, L., DUSAR, M., LEE, M., POITEVIN, C., ROYLES, C. & VERNIERS, J. 1993. A new look at Belgian aeromagnetic and gravity data through image-based display and integrated modelling techniques. *Geological Magazine* **130** (5): 583-591.

CHOVITZ, B. H., 1981 Modern geodetic earth reference models *EOS Transaction of the American Geophysical Union* 62: 65-67.

DEBACKER, T., SINTUBIN, M. & VERNIERS, J. 2004. Transitional geometries between gently plunging and steeply plunging folds: an example from the Lower Palaeozoic Brabant Massif, Anglo-Brabant deformation belt, Belgium. *Journal of the Geological Society***161**: 641-652.

DE VOS, W., POOT, B., HUS, J. & EL KHAYATI, M. 1992. Geophysical characterization of lithologies from the Brabant Massif as a contribution to gravimetric and magnetic modelling. *Bulletin de la Société belge de Géologie* **101** (3-4): 173-180.

DE VOS, W., VERNIERS, J., HERBOSCH, A. & VANGUESTAINE, M. 1993a. A new geological map of the Brabant Massif, Belgium. *Geological Magazine* **130** (5): 605-611.

DE VOS, W., CHACKSFIELD, B., D'HOOGE, L., DUSAR, M., LEE, M., POITEVIN, C., ROYLES, C., VANDENBORGH, T., VAN EYCK, J. & VERNIERS, J. 1993b. Image-based display of Belgian digital aeromagnetic and gravity data. *Geological Survey of Belgium Professional Paper* **263**.

DE VOS, W. 1997a. Geofysische en geologische aanwijzingen voor granietbatholieten in het Massief van Brabant. *Colloquium G.G.G. De diepe ondergrond in Vlaanderen,* Brussel.

DE VOS, W. 1997b. Influence of the granitic batholith of Flanders on Acadian and later deformation (Brabant Massif, Belgium). *Aardkundige Mededelingen* **8**: 49-52.

DE VOS, W. 1998. A short history of the pre-Variscan Brabant Massif, Belgium, from geological and geophysical evidence. Abstracts, Pre-Variscan terrane analysis of Gondwanan Europe. *Schr. Staatl. Mus. Min. Geol., Dresden,* **9**: 122-124.

DE VOS, W. & VERNIERS, J. 2000. New drillholes in the north-western Brabant Massif: confirmation of structures inferred from the aeromagnetic map. Abstract, Jos Bouckaert meeting of Geologica Belgica, 29.11.2000, Leuven.

DE MEYER, F. 1983. Gravity interpretation of the western flank of the Brabant Massif. *Koninklijk Meteorologisch Instituut, België, Publicaties serie A* (111): 1-34.

DE MEYER, F. 1984. Two structural models for the western flank of the Brabant Massif. *Geophysical Prospecting*, **32**: 37-50.

DOBRIN, M.B. 1976. Introduction to Geophysical Prospecting (third edition). McGraw-Hill Book Company.

DUQUENNE, H., EVERAERTS, M.& LAMBOT, Ph., 2005.Merging a Gravimetric Model of GPS/Leveling data: an example in Belgium.*Proceedings of the IAG Symposia*, Vol. 129: 131-136.

EVERAERTS, M. 2000. Interprétation structurale de la Manche au Rhin: l'apport du filtrage des champs potentiels. Thèse de doctorat, UCL, Louvain-la-Neuve.

EVERAERTS, M., POITEVIN, C., DE VOS, W. & STERPIN, M. 1996. Integrated geophysical/geological modelling of the western Brabant Massif and structural implications. *Bulletin de la Société belge de Géologie* 105 (1-2) : 41-59.

EVERAERTS, M., HENNEBERT, M., 1998.Interprétation des données gravimétriques de la zone frontalière franco-belge, entre Bailleul et Beaumont. *Annales de la Société géologique du Nord., T. 6 (2ème série) : 55-63.*

EVERAERTS, M., MANSY, J-L., 2001.Le filtrage des anomalies gravimétriques, une clé pour une compréhension des structures tectoniques du Boulonnais et de l'Artois (France). *Bulletin de la Société Géologique de France 172, n°3 : 267-274.*

EVERAERTS, M., LAMBOT, Ph., VAN HOOLST, T., VAN RUYMBEKE, M. & DUCARME, B., 2001.First-Order Gravity Network of Belgium. *Bulletin du Bureau Gravimétrique International*, No 89 : 27-41.

FRANCOIS, Ch., 1929 Recherches sur l'intensité de la pesanteur en Belgique. Annales de l'Observatoire de Belgique, 3e série tome 2 fasc.3, 150 pp, Uccle.

HEISKANEN, M., 1967.Physical geodesy. W H Freeman, San Francisco.

HENNEBERT, M. 1993. Rôle possible des structures profondes du Massif Cambro-Silurien du Brabant dans l'évolution des bassins sédimentaires post-Calédoniens (Belgique et Nord de la France). *Annales de la Société Géologique de Belgique* **116** (1) : 147-162.

JONES, L., 1948. Le levé gravimétrique de la Belgique (1947-1948). *Institut Géographique Militaire*, Bruxelles.

JONES, L., 1951. Les anomalies isostatiques en Belgique. ***Institut Géographique Militaire***, Bruxelles.

LEE, M.K. 1989. Upper crustal structure of the Lake District from modelling and image processing of potential field data. *British Geological Survey Technical Report* WK/89/1.

LEE, M., PHARAOH T., WILLIAMSON, J., GREEN, C. & DE VOS, W. 1993. Evidence of the deep structure of the Anglo-Brabant Massif from gravity and magnetic data. *Geological Magazine***130** (5) : 575-582.

LEGRAND, R. 1968. Le Massif du Brabant. *Memoirs of the Geological Survey of Belgium* **9**, 148 pp.

MANSY, J.L., LACQUEMENT, F., MEILLIEZ, F., HANNOT, F. & EVERAERTS, M., 1997. Interprétation d'un profil sismique pétrolier sur le méridien de Valenciennes (Nord de la France). *Aardkundige Mededelingen* **8** : 127-129.

MANSY, J.L., EVERAERTS, M.& DE VOS, W. 1999. Structural analysis of the adjacent Acadian and Variscan fold belts in Belgium and northern France from geophysical and geological evidence. *Tectonophysics* **309** : 99-116.

MATHERON, G. 1962-63. Traité de géostatistique appliquée, Eds Technip, France.

MELCHIOR, P. 1971. Physique et dynamique planétaire.4 volumes, Ed Vander, Louvain.

MOLODENSKY, M. S., 1967. Tides in an elastic rotating Earth with liquid core. In: Zemniye prilivy i vnutrennyeye stroeniye Zemli. Moscow. "Nauka", 3–9 (in Russian).

MORELLI, C., 1974. The gravity Standardization Net 1971 (IGSN71)*UGGI IAG Plub. Spéc*. (4) 194.

OULIDI, H.,1998Modèle géophysique de la croûte dans le nord de la France et en Belgique : étude de la limite sud du Massif du Brabant.Thèse de doctorat, UCL, Louvain-la-Neuve (unpublished PhD Thesis).

PAQUET, P., JIANG, Z. & EVERAERTS, M., 1997.A new Belgian geoid determination BJ96. *Proceedings of the Grageomar96 symposium, IAG*, Vol. 117: 605-612.

PEDLEY, R. (1991). GRAVMAG user manual: Interactive 2.5D gravity and magnetic modelling programme. British Geological Survey.

PHARAOH, T., MOLYNEUX, S., MERRIMAN, R., LEE, M. & VERNIERS, J. 1993. The Caledonides of the Anglo-Brabant Massif reviewed. *Special issue on the Caledonides of the Anglo-Brabant Massif. Geological Magazine***130** (5): 561-562.

PHARAOH, T., WINCHESTER, J., VERNIERS, J., LASSEN, A. & SEGHEDI, A. 2006. The Western Accretionary Margin of the East European Craton: an overview. *From GEE, D. & STEPHENSON, R. (eds), 2006. European Lithosphere Dynamics.* Geological Society, London, Memoir **32**: 291-312.

PIESSENS K., VANCAMPENHOUT P. & DE VOS W. 2005. Geologische subcropkaart van het

Massief van Brabant in Vlaanderen, 1/ 200 000. Belgische Geologische Dienst, Brussel, in opdracht van het Ministerie van de Vlaamse Gemeenschap, ANRE project VLA03-1.1.

RIJKERS, R., DUIN, E., DUSAR, M. & LANGENAEKER, V. 1993. Crustal structure of the London-Brabant Massif, southern North Sea. *Geological Magazine***130** (5): 569-574.

SCHWIDERSKI, E.W., 1980. Ocean Tides I, Global ocean tidal equations. *Marine Geodesy*, **3**: 161-217.

SKIBA, P., 2011. Homogene Schwerekarte der Bundesrepublik Deutschland (Bouguer Anomalien) Technischer Bericht zur Fortführung der Datenbasis, deren Auswertung und Visualisierung, 89 p, Leibniz-Institut für Angewandte Geophysik.

SINTUBIN, M. 1997a. Cleavage-fold relationships in the Lower Palaeozoic Brabant Massif (Belgium). *Aardkundige Mededelingen* **8**: 161-164.

SINTUBIN, M. 1997b. Structural implications of the aeromagnetic lineament geometry in the Lower Palaeozoic Brabant Massif (Belgium). *Aardkundige Mededelingen* **8**: 165-168.

SINTUBIN, M. 1999. Arcuate fold and cleavage patterns in the southeastern part of the Anglo-Brabant Fold Belt (Belgium): tectonic implications. *Tectonophysics*, **309**: 81-97.

SINTUBIN, M. & EVERAERTS, M. 2002. A compressional wedge model for the Lower Palaeozoic Anglo-Brabant Belt (Belgium), based on potential field data. *From:* WINCHESTER, J.A., PHARAOH, T.C. & VERNIERS, J. 2002, *Palaeozoic Amalgamation of Central Europe*. Geological Society, London, Special Publications, **201**: 327-343.

SIMPSON, R.W., JOCKEUS, R.C., BLAKELEY, R.J., SALTUS, R.W., 1986 A new isostatic residual gravity map of the conterminous United States with a discussion on the significance of isostatatic residual anomalies. *J. Geophys. Res.* 91: 8348-8372.

SOURIAU A. 1979. Upper mantle beneath the Paris Basin and Benelux, including possible volcanic anomalies in Belgium. *Tectonophysics* **57**: 167-188.

STRYKOWSKI, G., 1995 Borehole data and stochastic gravimetric inversion. PhDthesis,University of Copenhagen publication 4 series, vol. 3.

TELFORD, W.M., GELDART, L.P., AND SHERIFF,R.E., 1990 Applied Geophysics, *Cambridge University Press*.

VAN GROOTEL, G., VERNIERS, J., GEERKENS, B., LADURON, D., VERHAEREN, M.,HERTOGEN, J. & DE VOS, W. 1997. Timing of magmatism, foreland basin development, metamorphism and inversion in the Anglo-Brabant fold belt. *Geological Magazine*, **134** (5) : 607-616.

VERNIERS, W. & DE VOS, W. 1995. Recent research on the Brabant Massif. *Studia Geophysica et Geodaetica* **39** (3): 347-353, Prague.

VERNIERS, J., PHARAOH, T., ANDRE, L., DEBACKER, T., DE VOS, W., EVERAERTS, M., HERBOSCH, A., SAMUELSSON, J., SINTUBIN, M., VECOLI, M. 2002. The Cambrian to mid Devonian basin development and deformation history of Eastern Avalonia, east of the Midlands Microcraton: new data and a review. *In:* WINCHESTER, J.A., PHARAOH, T.C. & VERNIERS, J. (Eds.), *Palaeozoic Amalgamation of Central Europe*. Geological Society, London, Special Publications, **201**: 47-93.

WILLIAMSON, J.P., CHACKSFIELD, B., McEVOY, F., & PHARAOH, T. 2004. Reinterpretation of

gravity anomalies over the Brabant Massif in Southern Flandres (Belgium) Commissioned Report CR/04/215, British Geological Survey, Keyworth.